INCREMENTALLY ADAPTING GENERATIVE VISION-LANGUAGE MODELS WITH TASK CODEBOOK

Anonymous authors
Paper under double-blind review

ABSTRACT

With the help of large-scale pre-training, generative Vision-Language Models (VLMs) have acquired general-purpose capabilities. As downstream applications diversify, it is imperative for VLMs to learn and adapt continuously without experiencing catastrophic forgetting or necessitating complete retraining. In this work, we analyze the forgetting behavior of VLMs and propose a solution to enhance their incremental learning abilities. We introduce a Task Codebook within VLMs, enabling efficient retrieval of task-specific parameters for model adaptation. Our evaluation encompasses a diverse set of tasks spanning a wide range of visual domains and textual instructions. Experiments demonstrate that our approach effectively mitigates forgetting, even under highly demanding task sequences.

1 INTRODUCTION

Recent advancements in generative vision-language models OpenAI (2023); Alayrac et al. (2022); Chen et al. (2023c); Wang et al. (2022a); Google (2024) (VLMs) have demonstrated remarkable success. These models leverage extensive pre-training corpora to acquire substantial world knowledge, facilitating adaptation to downstream tasks. This paper investigates the *incremental learning* capabilities of such models. Our objective is to incrementally adapt generative VLMs to multiple tasks, rather than maintaining separate models specialized for each task.

A significant challenge in incremental learning is *catastrophic forgetting* McCloskey & Cohen (1989), where models rapidly lose previously learned knowledge. An ideal incrementally trained model should mitigate forgetting while retaining the ability to acquire new knowledge. Existing research has primarily focused on *class-incremental learning* for classification, assuming sequential availability of class subsets.

While class-incremental learning is an important research direction, general-purpose VLMs span a much wider set of applications than simple classification. It is thus more realistic to consider a *diverse* set of applications ranging from classification over detection to question answering. This poses a greater challenge for the incremental learning setting, as the model now needs to learn new applications instead of expanding a single application's coverage. More recent studies have examined catastrophic forgetting in vision-language models Garg et al. (2023); Zheng et al. (2023); Zhang et al. (2023). However, these methods often assume task similarity (e.g., different VQA tasks) He et al. (2023), limiting their practical applicability.

We propose a new incremental learning method for generative VLMs that improves their ability to learn and adapt to various, and potentially very different, tasks over time. To that end, we introduce a *task codebook* that stores *adapters* specialized for each encountered task. When presented with a new task, the model learns to access its most relevant modules to enhance its performance. This design allows our model to effectively learn diverse tasks without needing to know at inference time which task it is being asked to do, all while avoiding the common issue of *catastrophic forgetting* Compared to existing prompt-based solutions Wang et al. (2022c), we find that our method is more flexible and performs well across a wide set of incremental-learning settings.

To comprehensively evaluate the incremental learning capabilities of generative VLMs, we present a novel benchmark comprising diverse tasks, such as captioning Young et al. (2014); Gurari et al. (2020), VQA Goyal et al. (2017); Marino et al. (2019), OCR-enhanced captioning and VQA Sidorov et al. (2020); Wang et al. (2021), open-vocabulary classification Wang et al. (2022a), object detection Lin et al. (2014), referring expression generation Kazemzadeh et al. (2014), grounding Kazemzadeh et al. (2014) and multi-modal instruction tuning Liu et al. (2023). This diverse set of tasks enables a thorough assessment of incremental learning abilities under varying conditions, including different classes, datasets, and applications.

Our contributions in this paper can be summarized as follows:

- We propose a novel adaptation strategy for generative models with a task codebook that allows lookup and dynamic routing at inference time. This approach demonstrates efficacy in scenarios involving sequential tasks of different natures.
- We propose a new multi-modal incremental learning benchmark for generative models, spanning 36 datasets and 8 applications.
- We provide a comprehensive evaluation of our method under various scenarios, demonstrating our method's superiority over existing baselines across a wide range of tasks.

2 RELATED WORK

Incremental learning. In this task, the assumption is that the training set of a dataset is not available all at once. Data from previous timestamps are discarded as new data becomes available. Existing studies mainly focus on single modality such as images Hsu et al. (2018); Van de Ven & Tolias (2019) or texts Ke et al. (2023). For incremental learning in the vision domain, typical incremental learning setups include: task-incremental learning Hsu et al. (2018); Van de Ven & Tolias (2019), class-incremental learning Hsu et al. (2018); Van de Ven & Tolias (2019), domain-incremental learning Hsu et al. (2018); Van de Ven & Tolias (2019), task-agnostic incremental learning Aljundi et al. (2019a), and online continual learning Aljundi et al. (2019b).

Class-incremental learning. Existing approaches address this challenge through regularization techniques such as knowledge distillation Li & Hoiem (2017), model expansion Rusu et al. (2016); Wang et al. (2017) or representations Yan et al. (2021) and weight consolidation Aljundi et al. (2018); Chaudhry et al. (2018); Kirkpatrick et al. (2017). Alternatively, replay-based methods retain a small sample of data from previous classes Rebuffi et al. (2017); Chaudhry et al. (2019); Iscen et al. (2020). More recent techniques introduce prompt retrieval for class-incremental learning Wang et al. (2022c;b); Khan et al. (2023); Tang et al. (2023) without requiring a replay buffer.

Multi-modal incremental learning. Multi-modal incremental learning has seen recent interest due to the advancement of multi-modal models Radford et al. (2021); Wang et al. (2022a); Li et al. (2023). Some of the research has focused on dual-encoder models, *e.g*. CLIP Radford et al. (2021), examining their performance on evolving data distributions Garg et al. (2023) and knowledge preservation Zheng et al. (2023). Other studies focus on incremental learning for the Visual-Question Answering (VQA) tasks, either by formulating it as a classification problem Qian et al. (2023); Srinivasan et al. (2022) or a generative task Zhang et al. (2023); He et al. (2023). In this paper, we adopt a more practical setting with varied tasks and leverage generative models like GIT Wang et al. (2022a) for their potential across diverse settings.

Codebook learning. Codebook learning is an effective method for converting continuous features into semantically rich, discrete codes. This technique has found widespread application in the field of self-supervised representation learning Caron et al. (2020; 2021) and reconstruction Van Den Oord et al. (2017); Ramesh et al. (2021). Inspired by recent advancements in retrieval mechanisms that facilitate incremental learning in classifiers Prabhu et al. (2023); Wang et al. (2022c;b), this study introduces the concept of a task codebook. Our approach enables sequential task learning in a non-interfering manner, effectively addressing the challenge of catastrophic forgetting.

3 METHOD

Our goal is to incrementally adapt a generic auto-regressive model to various challenging (and potentially very diverse) image-to-text tasks. In this section, we start by defining the task incremental learning setup before describing our proposed task codebook incremental adaptation (TCIA) method.

3.1 PROBLEM SETUP

Auto-regressive vision-language models form the building blocks of most state-of-the-art systems for challenging image-to-text tasks Chen et al. (2023b). While a large body of work has focused on efficient ways to adapt these models to different tasks Hu et al. (2021); Lester et al. (2021); Li & Liang (2021), we explore in this work how to adapt them to a sequential stream of tasks, in an

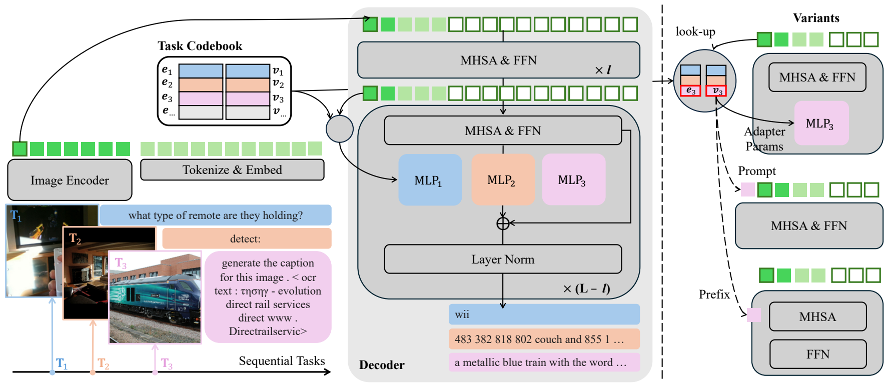
Task Codebook
Image Encoder
Tokenize & Embed
what type of remote are they holding?
detect:
generate the caption for this image . < ocr text : τησηγ - evolution direct rail services direct www . Directrailservic>
Sequential Tasks
MHSA & FFN
× l
Layer Norm
× (L − l)
Decoder
wii
483 382 818 802 couch and 855 1 …
a metallic blue train with the word …
look-up
Variants
Adapter Params
Prompt
Prefix
MHSA
FFN

Figure 1: **Overview of TCIA**. We introduce a task codebook in a generic auto-regressive generative model. Task-specific codebook keys are used to retrieve task-specific codebook values, which are adapter MLP parameters Houlsby et al. (2019) by default (**left**). We also consider prompt Lester et al. (2021); Wang et al. (2022c) or prefix Li & Liang (2021) as alternative ways to condition the model into different tasks (**right**).

incremental manner. Formally, let us consider a task mixture $\mathbf{T}$ of T different tasks: a data sample for each task $t \in \mathbf{T}$ is represented as $x \sim \mathcal{D}_t$, such that $x = (x_v, x_i, y) \sim (\mathcal{V}_t, \mathcal{I}_t, \mathcal{Y}_t)$, where $\mathcal{V}_t$, $\mathcal{I}_t$ and $\mathcal{Y}_t$ respectively denote the visual input, textual instruction input and textual target output spaces of this task. For example, when considering a VQA task, $\mathcal{V}_t$ represents images, $\mathcal{I}_t$ questions and $\mathcal{Y}_t$ expected answers for this task.

Typically, models are adapted to each task t individually, hence resulting in a collection of T specialized models. We refer to this strategy as *single-tasking*. On the other hand, it is also common to train a single model on the entire task mixture $\mathbf{T}$ at once by, for example, randomly sampling a different task from the mixture each step. We refer this as *multi-tasking*. In this work, we consider another scenario where tasks come in a sequential manner. This mirrors real-world conditions where practitioners adapt a single model on the fly due to the unavailability of all tasks upfront.

Sequential tasks. We consider the scenario where tasks arrive sequentially, requiring continuous adaptation of a single model. Specifically, for task t, we assume access solely to $\mathcal{D}_t$ (data from the corresponding task), and not to $\mathcal{D}_i$ for any $i \neq t$ (data from the other tasks). The challenge of this *incremental learning* setup is to learn over the different tasks while mitigating *catastrophic forgetting*. In contrast to previous incremental learning methods focusing on incrementally growing label spaces for image recognition Wang et al. (2022b;c), we assume that the nature of the task and the data distribution $\mathcal{D}_t$ can vary significantly across tasks.

Auto-regressive generative models. Since our goal is to solve a mixture of image-to-text tasks, we build upon standard auto-regressive generative vision-language models Wang et al. (2022a). Formally, let us consider an input image-text data pair $x = (x_v, x_i) \sim (\mathcal{V}_t, \mathcal{I}_t)$ from task t. It is transformed into a set of N d-dimensional embeddings $\mathbf{X} \in \mathbb{R}^{N \times d}$ formed by concatenating the output of a visual encoder processing x_v and a text tokenizer processing x_i. We use an auto-regressive text decoder $g(\cdot)$ with L layers to generate the target text $y \in \mathcal{Y}_t$. Specifically, the decoder predicts each text token y_k from the target text (we denote its length by K) given both the set of preceding token embeddings $\mathbf{Y}_{<k}$ and the input image-text pair embeddings $\mathbf{X}$. We train with a language modeling objective:

$$\mathcal{L} = \frac{1}{K} \sum_{i=1}^{K} \ell(y_k, g([\mathbf{X}; \mathbf{Y}_{y_{<k}}]))$$

where $[;]$ corresponds to the concatenation operation in the first dimension and ℓ is the softmax cross-entropy loss with label-smoothing Müller et al. (2019). We average this loss over minibatches of examples drawn in $(x_v, x_i, y) \sim (\mathcal{V}_t, \mathcal{I}_t, \mathcal{Y}_t)$.

3.2 Task Codebook Incremental Adaptation (TCIA)

Incremental learning often employs buffer replay, using either past input data Chaudhry et al. (2019) or past model weights Li & Hoiem (2017) to mitigate catastrophic forgetting. However, storing extensive data or numerous model replicas becomes infeasible as task and model scales increase. In this paper, we introduce a novel task codebook method using task-specific keys and values. The task keys are efficiently retrieved using a nearest neighbor lookup mechanism and dynamically updated. Each retrieved task key is paired with a task value, which is then employed to efficiently condition the remaining layers of the model Lester et al. (2021); Li & Liang (2021); Houlsby et al. (2019) to the considered task. This design choice effectively integrates our task lookup module within the decoder, enabling the deeper generative layers to adapt to a diverse set of tasks. An overview of our method is presented in Fig. 1.

Task codebook. Formally, we introduce a task codebook at the l^{th} decoder layer of the generative model. This codebook contains a key-value pair $(\boldsymbol{e}_t, \boldsymbol{v}_t)$ for each task t of the task mixture $\mathbf{T}$. The task-specific keys $\boldsymbol{e}_t \in \mathbb{R}^d$ are used to recognize which task to be dealt with while the task-specific values $\boldsymbol{v}_t$ are employed to adapt the last $N_l = L - l$ layers of the model to the considered task.

Task-specific keys: recognizing tasks with lookups. Intuitively, we want a task-specific key $\boldsymbol{e}_t$ to be able to recognize which task t we are currently solving, making it play the role of a *prototype* for task t. A simple yet effective strategy to do so is to use an average of the input embeddings coming from the considered task t. Specifically, at training time, we dynamically update the relevant task keys with an exponential moving average (EMA) of the sequence representation at the l^{th} decoder layer, denoted by $\mathbf{x}^l$, coming from examples sampled from $\mathcal{D}_t$. Formally, we have for each task t: $\boldsymbol{e}_t = m \cdot \boldsymbol{e}_t + (1 - m) \cdot \mathbf{x}^l$ where $\mathbf{x}^l$ is the embedding of an example $x = (x_v, x_i) \sim (\mathcal{V}_t, \mathcal{I}_t)$ sampled from task t and m is a decay rate. An alternative is to learn the task keys via gradient descent using an additional loss term as in L2P Wang et al. (2022c). Our simple EMA design offers faster adaptation and results in improved performance compared to learning the keys (see Sec. 5.5). We empirically find that max-pooling exhibits robust advantages across all learning setups when it comes to the choice of the sequence representation (see also Sec. 5.5).

At inference time, we simply select a relevant task index t for the evaluated input x by performing a nearest-neighbor lookup, defined as $t = \text{argmax}_i \gamma(\boldsymbol{e}_i, \mathbf{X}^l_0)$ where γ is a similarity metric. In practice, we use cosine similarity.

Task-specific values: parameter-efficient adaptation. In order to achieve efficient adaptation to each task and minimal parameter overhead, we integrate the task-specific values $\boldsymbol{v}_t$ as parameters within an *adapter* module Houlsby et al. (2019). Specifically, the task-specific values $\boldsymbol{v}_t$ represent a set of N_l lightweight bottleneck multi-layer perceptron (MLP) parameters introduced after the attention and feedforward layers of each of the last N_l transformer decoder blocks. We refer to this way of adapting the decoder using task-specific MLPs by the *adapter* strategy and denote the resulting model by TCIA$^{\text{A}}$. As illustrated in the right panel of Fig. 1, we also evaluate alternative strategies denoted by TCIA$^{\text{P}}$ (resp. TCIA$^{\text{Pr}}$) where task-specific values $\boldsymbol{v}_t$ refer instead to a prompt Lester et al. (2021); Wang et al. (2022c) (resp. to a prefix Li & Liang (2021)). We find in our experiments (see Tab. 1) that while these two variants perform competitively and strongly allievate forgetting, our variant using adapters, *i.e.* TCIA$^{\text{A}}$, leads to the best version of our task codebook incremental adaptation framework.

3.3 Implementation Details

Auto-regressive model. We build upon GiT-Large Wang et al. (2022a), a decoder-only auto-regressive model with 400M parameters. The image encoder is initialized from CLIP-L/14 Radford et al. (2021) and we use a 6-layer text decoder with internal dimension $d = 768$. Our model is first pre-trained jointly on WebLI-100M Chen et al. (2023c) and Conceptual Captions-12M Sharma et al. (2018) as a general image captioner.

Task codebook. We insert the task codebook before the first layer of the decoder, *i.e.* we have $l = 0$. For adapters Houlsby et al. (2019), we use two 2-layer MLP modules with an internal dimension $s = 256$, resulting in a parameter increase of $N^l \times T \times 2(2ds + s + d)$. The parameter count increase for the other variants of TCIA are $N^l \times T \times ds$ for TCIA$^{\text{P}}$ and $N^l \times T \times 2ds$ for TCIA$^{\text{Pr}}$. The decay rate m is set to 0.99 by default.

Upper-bounds. Our upper-bounds are *single-tasking* and *multi-tasking*. These variants do not adapt the model sequentially, but either train multiple specialized models (single-tasking) or a general model with all tasks at once (multi-tasking).

Baselines. For sequential task learning, we consider a simple baseline which consists in simply fine-tuning the model to different tasks in a sequential manner. This usually leads to catastrophic forgetting. Episodic Replay (E-Replay) Chaudhry et al. (2019) is another baseline where we store

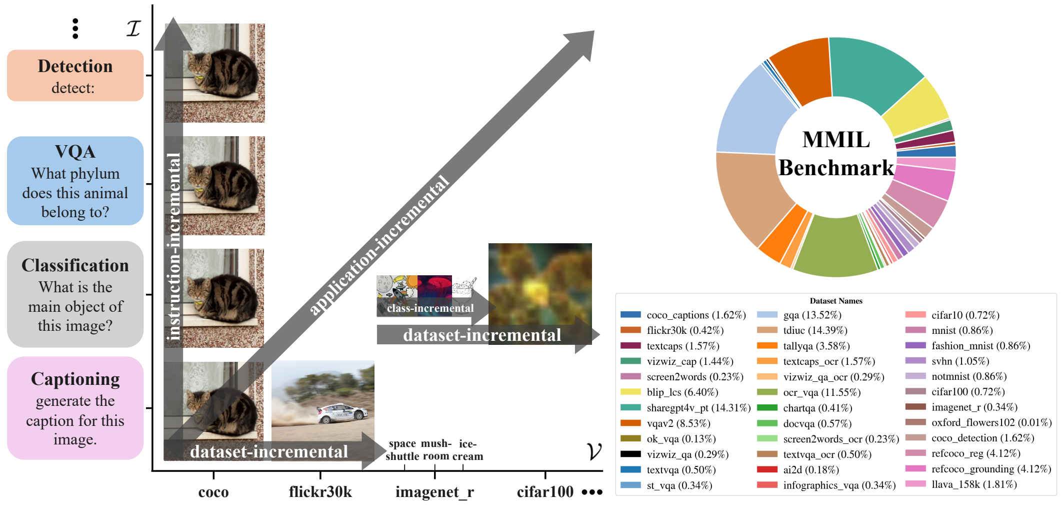

Figure 2: **Multi-Modal Incremental Learning (MMIL) benchmark** consists of 36 datasets across 8 applications (**left**) and 4 incremental learning setups (**right**).

previous samples in a memory buffer to re-use when learning new tasks. This constitutes a strong and effective baseline for sequential tasks. We use 1% of the entire dataset as the size of the memory buffer by default, similar to He et al. (2023). Finally, we extend L2P Wang et al. (2022c), a state-of-the-art incremental learning method designed for classification, to our multi-modal benchmark , by using the concatenated visual feature and textual instruction feature from CLIP-B Radford et al. (2021) as the *key*. We call it L2P+. Prompts are then retrieved from the pool and used as additional input to the decoder.

4 Multi-Modal Incremental Learning Benchmark

In this section, we first introduce the comprehensive set of tasks employed in our benchmark. We then define different incremental learning paradigms utilized in our experiments. A schematic diagram is demonstrated in Fig. 2.

4.1 Applications

To assess the adaptability of VLMs in addressing a wide set of applications, we curate a benchmark of 8 multi-modal applications, including *captioning*, *VQA*, *OCR-CV*, *classification*, *detection*, *referring expression*, *grounding*, and *multi-modal instruction tuning*, across a total of 36 datasets. These applications span a wide range of visual and textual domains detailed in Appendix A.1 and Tab. 7.

4.2 Incremental-Learning Setups

In Sec. 3, we describe our method which adapts the model for each task t in a task mixture $\mathbf{T}$. We now define various incremental-learning setups with differing definitions for the mixture $\mathbf{T}$ and showcase their connections in Fig. 2.

Dataset-incremental learning. In this setup, we define each task t as a single dataset. The task mixture $\mathbf{T}$ refers to the union of different datasets within the same application. For example, classification is an application and CIFAR-100 and ImageNet-R datasets are different tasks for this application.

Class-incremental learning. This is the traditional incremental classification setup Wang et al. (2022c;b); Khan et al. (2023), where each task t refers to a subset of classes of a classification dataset. The entire task mixture $\mathbf{T}$ corresponds to a single dataset, such as CIFAR-100 in this scenario.

Instruction-incremental learning. We fix the visual input set $\mathcal{V}$ in this scenario and incrementally modify the textual input $\mathcal{I}$ over different tasks. We use the COCO dataset Lin et al. (2014) and adapt the model with different textual instructions in each task t. Different variations of textual instructions include captioning, VQA (OK-VQA Marino et al. (2019)), object detection, referring expressions (RefCOCO Kazemzadeh et al. (2014)) and grounding (RefCOCO Kazemzadeh et al. (2014)). The respective textual inputs for these five tasks are the following: *"Generate the caption for this image."*,

Table 1: **Dataset-incremental learning** where different tasks correspond to different datasets of the same application. The considered applications are captioning, VQA, OCR-CV, and classification. *F* and *Acc.* denote forgetting and average accuracy at the end of training. All numbers are run by us.

	Captioning		VQA		OCR-CV		Classification	
Method	F↓	Score ↑	F↓	Score ↑	F↓	Score ↑	F↓	Score ↑
Single-tasking								
Finetuning	–	121.4	–	56.7	–	49.1	–	97.1
Adapter	–	104.7	–	56.4	–	48.4	–	94.7
Multi-tasking								
Finetuning	–	112.9	–	59.4	–	40.4	–	96.9
Adapter	–	96.9	–	56.8	–	37.4	–	93.8
Sequential tasks								
Finetuning	26.4	62.3	7.97	42.4	20.4	14.8	71.3	24.2
Adapter	12.1	57.5	13.6	36.4	20.1	9.63	82.0	11.9
E-Replay	15.9	77.3	3.67	52.7	4.25	30.3	23.0	67.0
L2P+	3.14	83.2	0.55	48.9	1.50	35.4	0.39	90.8
TCIA$^{\text{P}}$ (Ours)	0.66	79.4	0.66	50.7	0.38	35.3	0.08	90.9
TCIA$^{\text{Pr}}$ (Ours)	0.84	88.1	0.93	53.2	**0.23**	39.2	**0.06**	92.5
TCIA$^{\text{A}}$ (Ours)	**0.47**	**100.8**	**0.54**	**55.1**	0.31	**45.7**	0.15	**94.0**

"<question>", *"detect:"*, *"describe the box at <location>"* and *"detect <object>:"*. Overall, the task mixture $\mathbf{T}$ is the COCO dataset seen five times, each associated with textual inputs of a different nature.

Application-incremental learning. This setup increments over different *applications*. For each task t, we adapt the model to a specific application, *e.g*. VQA, by training on the combined datasets corresponding to that application. The union of all tasks *i.e*. $\mathbf{T}$ refers to the combination of 8 applications (see Section 4.1) in this scenario.

4.3 Metrics

To evaluate the efficacy of TCIA and the baseline methods, we employ distinct metrics appropriate to each dataset and application. We report the average of all the metrics across different datasets and tasks as correctness *score* (higher is better). We also report the widely-used *forgetting* metric Chaudhry et al. (2018) (denoted by F in our experiments), which quantifies the extent to which a model has forgotten a task based on its current state. See Appendix A.4 for detailed definition.

5 Experiments

In this section, we first assess the performance of our proposed TCIA framework on the different incremental learning setups described in Sec. 4.2. Second, we show an ablation study of different important components of TCIA. Finally, we identify potential areas of improvement for our model by analyzing the performance of an oracle model that always chooses the right task at inference.

5.1 Dataset-Incremental Learning

We conduct dataset-incremental learning across 4 diverse applications. These applications are all comprised of different datasets as detailed in Tab. 7.

Baseline comparison. We see in Tab. 1 that TCIA models outperform all the considered baselines in the sequential task learning scenario. First, as expected, the naive baseline of training the model directly on sequential tasks yields severe forgetting: for example we observe -59.1 points of performance drop on captioning compared to single-tasking for finetuning. Second, we see that the strong E-Replay Chaudhry et al. (2019) and L2P+ Wang et al. (2022c) baselines alleviate partly the forgetting but still suffer from performance degeneration. The two main design differences between TCIA$^{\text{P}}$ and L2P+ methods are (i) exponential moving average (EMA) versus gradient back-propagation to update the task-specific keys and (ii) the task-specific keys are built from decoder inner layers rather than off-the-shelf backbones Dosovitskiy et al. (2020). We validate in Tab. 6i that our design choices are favorable. Details of incremental learning scores across training steps are provided in the Fig. 6. Overall, our TCIA models improve over strong baselines for incremental learning, especially on complex multi-modal benchmarks.

Table 2: **State-of-the-art comparison in class-incremental learning.** 10 class splits of CIFAR100 Krizhevsky et al. (2009); Wang et al. (2022c) and Split ImageNet-R Wang et al. (2022b) are considered. *Add. Models* denotes the additional models used. For E-Replay Chaudhry et al. (2019), we specify the size of the memory buffer in parenthesis. For reference, we also report the upper bound by training on the entire dataset, corresponding to *multi-tasking*. We bold best results within the two studied model size categories: *base* and *large*.

	Method	Model	Add. Models	Split CIFAR100		Split ImageNet-R	
				F↓	Score ↑	F↓	Score ↑
Base	Upper-bound	ViT-B	–	–	90.9	–	79.1
	Upper-bound	GiT-B	–	–	85.9	–	80.0
	E-Replay (1k)	ViT-B	–	33.3	67.9	35.4	55.1
	E-Replay (5k)	ViT-B	–	16.5	82.5	23.3	65.2
	L2P	ViT-B	ViT-B Dosovitskiy et al. (2020)	7.35	83.9	9.73	61.6
	DualPrompt	ViT-B	ViT-B Dosovitskiy et al. (2020)	5.16	86.5	4.68	68.1
	LGCL	ViT-B	VIT-B Dosovitskiy et al. (2020) & CLIP-B Radford et al. (2021)	**5.10**	**87.2**	4.20	69.5
	TCIA	GiT-B	ViT-B Dosovitskiy et al. (2020)	9.25	84.6	**3.70**	**72.9**
Large	Upper-bound	GiT-L	–	–	94.1	–	93.5
	E-Replay (5k)	GiT-L	–	12.9	84.9	12.5	71.5
	TCIA	GiT-L	–	10.2	81.7	12.1	59.5
	TCIA	GiT-L	ViT-B Dosovitskiy et al. (2020)	**9.16**	**87.0**	**3.02**	**77.6**

Different TCIA variants. We observe in the last three rows of Tab. 1 that our model with adapters (TCIA$^{\mathrm{A}}$) leads to better performance across different dataset-incremental learning benchmarks. The superiority of the adapter variant compared to prompt or prefix variants is mainly explained by the stronger transfer capability of the adapter module in general. Interestingly, we observe that TCIA$^{\mathrm{P}}$ and TCIA$^{\mathrm{Pr}}$ models also perform strongly and exhibit low forgetting. This shows that our TCIA framework is robust to the choice of adaptation method. In the following experiments, we stick to the best performing TCIA$^{\mathrm{A}}$ variant and denote it as TCIA for brevity.

5.2 Class-Incremental Learning

Further, We apply our TCIA framework to the standard class-incremental learning scenario. This allows us to compare our results with previously published numbers. Note that unlike existing methods Wang et al. (2022c); Khan et al. (2023), TCIA is not designed specifically for discriminative classification tasks. Yet, we show that our generative TCIA model is still effective and performs decently well. To tailor our method for classification, we further consider using features from an additional model (*Add. Model*) to learn task key representation. We further consider varying class splits in the Appendix B.2, showcasing the unique advantage of TCIA when class splits increase.

Comparison with the state of the art. We compare TCIA to previously published results in the traditional setting of class-incremental learning on CIFAR-100 and Split ImageNet-R Wang et al. (2022c). In Tab. 2, we see that TCIA reaches competitive performance with recent state-of-the-art class-incremental learning, though it is not specifically designed for this scenario. Notably, we improve over previously published work Khan et al. (2023) on Split ImageNet-R by +8.1 points (77.6 *v.s.* 69.5). Our performance on CIFAR100 is competitive but remains -0.2 points behind the state of the art (87.0 *v.s.* 87.2), likely because CIFAR100 is a small dataset with limited visual and task complexity and hence does not benefit from the potential of adapting large multi-modal models. TCIA exhibit less forgetting compared to the E-Replay baseline as an increasing amount of classes are presented, especially for a more complicated dataset like Split ImageNet-R.

5.3 Instruction-incremental learning

In this experiment, we consider the instruction-incremental learning setup as detailed under the corresponding paragraph in Sec. 4.2. The goal is to incrementally learn to perform different tasks, namely captioning, VQA, object detection, referring expressions and grounding, *on the same set of images*. For all the entries in Tab. 3, we train the model with 60K iterations and a batch size of 1024. We see in Tab. 3 that TCIA performs favorably against E-Replay Chaudhry et al. (2019) (+6.1 points) and L2P+ baselines (+8.9 points), exhibiting minimal forgetting. Notably, our model almost closes the gap with the multi-tasking upper-bound with only 1.5 points of performance drop (60.6 *v.s.* 62.1).

Table 3: **Instruction-incremental learning** on COCO Lin et al. (2014) dataset with 5 different textual instructions and same visual input.

Method	F↓	Score ↑
Multi-tasking		
Finetuning	–	66.8
Adapter	–	62.1
Sequential tasks		
E-Replay	13.7	53.9
L2P+	0.47	51.1
TCIA	**0.24**	**60.6**

Table 4: **Application-incremental learning** on 8 applications (*App.*) across 36 datasets (*Data.*).

Method	Score ↑	
	8 App.	36 Data.
Multi-tasking		
Finetuning	72.7	
Adapter	63.7	
Sequential tasks		
E-Replay	57.7	53.9
L2P+	49.3	48.2
TCIA	**59.2**	**67.2**

5.4 Application-incremental learning

Lastly, in Tab. Tab. 4, we conduct experiments on the most challenging learning setup in terms of both task diversity as well as task quantity. We curate a list of 8 applications consisting of 36 datasets, detailed in the Tab. 7, and evaluate the model's capacity in learning incrementally across very diverse visual and textual instruction input. We consider two settings: (i) each application is taken as a task with different datasets within that application combined directly (8 *App.* with 8 tasks in total) and (ii) each dataset is taken as a task (36 *Data.* with 36 tasks in total). For all entries in Tab. Tab. 4, we train the model with 400K iterations with a batch size of 1024. Our results with TCIA outperform E-Replay Chaudhry et al. (2019) by a large margin of +1.5 points and +14.3 points on two settings, respectively. This challenging setting validates our method's effectiveness in alleviating forgetting in realistic incremental learning environments. Notably, TCIA with 36 task codes outperforms the multi-tasking adapter baseline by +3.5 points (67.2 *v.s.* 63.7). This suggests that the proposed task codebook not only helps alleviate forgetting but also improves final performance upper-bound.

5.5 Ablation Study

In this section, we thoroughly analyze TCIA to assess the impact of each component. To complement the end-task incremental learning score, we introduce an additional metric, Acc_{L}, which directly quantifies the lookup module's performance by measuring the accuracy of selecting the correct task key during inference.

Task key representation. We study the impact of different task key representations on codebook lookup accuracy (Tabs. 5i and 5ii) and end-task incremental learning score (Tab. 5iii). We find that using *max-pooling* over the sequence feature yields robust lookup accuracy over different incremental learning setups. This echos studies on text classification Chen (2015); Conneau et al. (2017) finding that max-pooling excels at capturing salient information for tasks like sentiment analysis where the presence of certain keywords is informative. Notably, we find that `[CLS]` and `[EOS]` are complementary-`[CLS]` excels at dataset-incremental learning while `[EOS]` excels at instruction-incremental learning. Although their concatenation offers higher lookup accuracy hence end-task score, it still lags behind from simply using max-pooling. See Tab. 17 for additional results on other setups.

Task codebook depth. We incorporate the task codebook into the l-th decoder layer, effectively adapting the subsequent $N - l$ layers. We use a GiT decoder with $N = 6$ layers and investigate the impact of task codebook depth by varying l in Tabs. 5i and 5ii. Results indicate that positioning the codebook at the shallowest layer ($l = 0$) performs more robustly against an intermediate placement ($l \geq 1$) when using max-pooling as task key representation. For models with the task codebook placed at deeper layers, the end-task score decline is primarily attributed to low Acc_{L}, suggesting that the model struggles to identify the appropriate task key at inference.

Update strategy. We discuss two alternatives to update the task-specific keys described in Section 3.2. As shown in Tab. 6i, employing Exponential Moving Average (EMA) with $m = 0.99$ for task code updates yields a higher performance for both captioning and VQA. In comparison to learning the keys via gradient backpropagation as in L2P approach Wang et al. (2022c), we observe improvements of +2.4 points and +1.1 points on captioning and VQA, respectively.

Table 5: **Ablation study** on different choices of task key representations (*Rep.*) and task codebook depth l. **Left:** Task codebook lookup accuracy (Acc_L) with the default setup <u>underlined</u>. **Right:** incremental learning score with the optimal l. Task key representations including (a) `[CLS]`; (b) `[EOS]`; (c) `[[CLS];[EOS]]`; (d) mean-pooling; (e) max-pooling; (f) `[[CLS];`max-pooling`]`; (g) `[[CLS];[EOS];`max-pooling`]` (h) CLIP-B Radford et al. (2021) are ablated.

l	(a)	(b)	(c)	(d)	(e)	(f)	(g)	(h)
0	45.7	93.7	95.3	49.2	<u>94.6</u>	87.3	95.0	89.5
1	46.9	92.0	96.0	62.2	95.1	83.0	94.6	89.5
2	66.6	91.3	95.4	66.9	96.2	96.0	95.0	89.5
3	83.7	92.9	95.2	86.6	94.7	90.8	96.3	89.5

(i) $\textbf{Acc}_\textbf{L}$**.** Dataset-incremental learning on VQA datasets.

l	(a)	(b)	(c)	(d)	(e)	(f)	(g)	(h)
0	53.6	40.2	80.5	58.9	<u>96.9</u>	87.6	82.6	71.3
1	59.7	42.2	81.4	66.9	94.3	85.9	83.1	71.3
2	72.1	51.5	82.7	74.1	87.0	83.3	85.0	71.3
3	79.3	54.8	82.1	74.6	82.8	83.2	85.6	71.3

(ii) $\textbf{Acc}_\textbf{L}$**.** Application-incremental learning on 36 datasets.

Rep.	Data.		Inst.	App.
	Cap.	VQA		
(a)	90.6	45.9	35.7	49.7
(b)	64.2	55.1	58.9	31.3
(c)	97.4	55.1	58.2	53.7
(d)	91.2	47.8	46.8	50.1
(e)	**100.8**	55.1	**60.6**	**67.2**
(f)	92.8	54.0	57.2	59.9
(g)	97.8	**55.2**	**60.6**	55.8
(h)	94.3	53.2	**60.6**	51.4

(iii) **Incremental learning score**. *Data.*, *Inst.*, and *App.* denotes dataset-, instruction-, and application-incremental learning setup, respectively.

Table 6: **Ablation study** on the design of the update strategy (**left**), internal dimensionality (**middle**), and adaptation strategy (**right**) of the task codebook. We report the task score. +*Param.* refers to the ratio of additional parameters introduced by TCIA compared to the entire model *per layer per task*.

Update	m	Cap.	VQA
Backprop	–	98.4	54.0
EMA	0.97	98.3	54.9
EMA	0.99	**100.8**	**55.1**
EMA	0.996	100.0	54.4

(i)

s	+Param.	Cap.	VQA
128	0.1%	98.0	55.0
256	0.2%	**100.8**	**55.1**
512	0.4%	98.0	54.3

(ii)

Attn.	MLP	+Param.	Cap.	VQA
✓		0.1%	96.8	54.9
	✓	0.1%	99.0	55.0
✓	✓	0.2%	**100.8**	**55.1**

(iii)

Internal dimensionality. As described in Sec. 3.2, TCIA^A incorporates adapter-based task-specific values consisting of 2-layer MLPs with internal dimensionality s. In Tab. 6ii, we assess the impact of this parameter s both in terms of performance and parameter count increase. Our results show that a value of $s = 256$ offers an optimal balance between accuracy and memory consumption. Beyond this point, performance gains start to saturate, while the memory footprint keeps increasing.

Adaptation strategy. By default, we use two 2-layer MLPs to adapt the generative model, one after the self-attention (*Attn.*) layer and the other after the MLP layer Houlsby et al. (2019). We explore whether the memory consumption can be further decreased by discarding either one of the two 2-layer MLPs. Results in Tab. 6iii indicate that adapting with two placements achieves optimal results.

5.6 Analysis

Confusion Matrix. We study the task key selection accuracy (Acc_L) further by showcasing the confusion matrix between different datasets. In Fig. 3, we observe that the model can mostly retrieve the correct task-specific key (*i.e.*, 96.9% accuracy). TextVQA Singh et al. (2019) in the OCR-CV application is mostly easily confused with TDIUC Kafle & Kanan (2017) in the VQA application. Fashion-MNIST Xiao et al. (2017) and NotMNIST Bulatov (2011) in the classification application are sometimes confused with COCO Lin et al. (2014) in the detection application and ChartQA Masry et al. (2022) in the OCR-CV application.

Oracle. We present in Fig. 4 the performance of TCIA in the presence of an oracle, *i.e.* selecting the ground-truth task key at inference time. This assesses the potential performance gains we could have with better task lookup designs and represents an upper-bound for TCIA. Interestingly, we observe that there are still potential gains by improving the task-specific lookup accuracy: *i.e.* +10.9 points on CIFAR-100 and +6.6 points on 8 applications. On the other hand, there is virtually no gain by having an oracle in VQA dataset incremental learning setup since Acc_L is already very high (94.6%

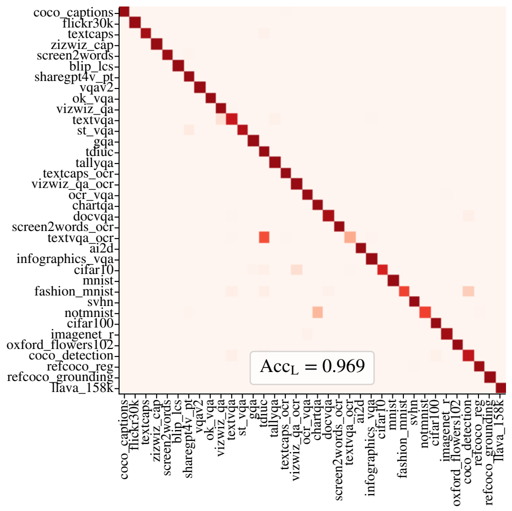

Figure 3: **Confusion matrix** for application-incremental learning across 36 datasets.

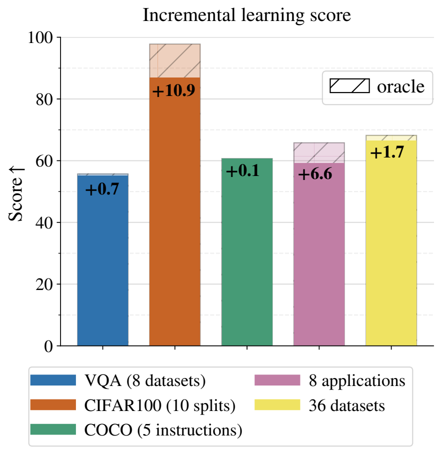

Figure 4: **Performance improvements** in terms of incremental learning score when considering an oracle retrieving the correct task at inference time.

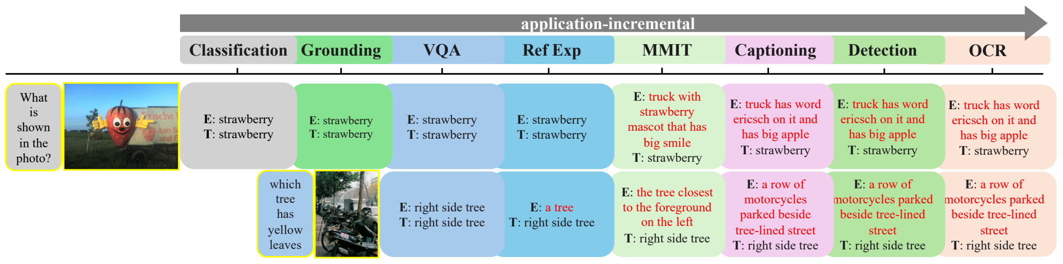
application-incremental
Classification
Grounding
VQA
Ref Exp
MMIT
Captioning
Detection
OCR
What is shown in the photo?
E: strawberry T: strawberry
E: strawberry T: strawberry
E: strawberry T: strawberry
E: strawberry T: strawberry
E: truck with strawberry mascot that has big smile T: strawberry
E: truck has word ericsch on it and has big apple T: strawberry
E: truck has word ericsch on it and has big apple T: strawberry
E: truck has word ericsch on it and has big apple T: strawberry
which tree has yellow leaves
E: right side tree T: right side tree
E: a tree T: right side tree
E: the tree closest to the foreground on the left T: right side tree
E: a row of motorcycles parked beside tree-lined street T: right side tree
E: a row of motorcycles parked beside tree-lined street T: right side tree
E: a row of motorcycles parked beside tree-lined street T: right side tree

Figure 5: **Qualitative comparison** between TCIA (T) and E-Replay Chaudhry et al. (2019) (E) with incremental learning on 8 applications.

accuracy). This suggests that further enhancements in task lookup accuracy could lead to substantial performance gains and is a promising direction for future work.

Qualitative Analysis. We showcase in Fig. 5 the qualitative comparison of the forgetting behaviour between TCIA and the E-Replay method Chaudhry et al. (2019). Comparatively, the output from E-Replay is more prone to drift from ground truth after subsequent tasks are finished. For example, after being fine-tuned on the MMIT application, E-Replay mistakenly predicts "*truck with strawberry mascot that has big smile*", while TCIA robustly predicts the label name of the image "*strawberry*".

6 Conclusion

In this paper, we expand the setting of incremental learning to the scope of VLMs. With a high diversity of tasks, datasets and modalities, we model a realistic setting of adapting large multi-modal models for various downstream applications while minimizing forgetting. We introduce a new simple incremental learning method, TCIA, that improves over prior proposed methods and baselines, especially for complex tasks. We extensively evaluate our new incremental learning method on 36 datasets and 8 applications. We hope that our paper will help the community to advance incremental learning research for large multi-modal models.

REFERENCES

Manoj Acharya, Kushal Kafle, and Christopher Kanan. Tallyqa: Answering complex counting questions. In *AAAI*, 2019.

Jean-Baptiste Alayrac, Jeff Donahue, Pauline Luc, Antoine Miech, Iain Barr, Yana Hasson, Karel Lenc, Arthur Mensch, Katherine Millican, Malcolm Reynolds, et al. Flamingo: a visual language model for few-shot learning. *Advances in Neural Information Processing Systems*, 35:23716–23736, 2022.

Rahaf Aljundi, Francesca Babiloni, Mohamed Elhoseiny, Marcus Rohrbach, and Tinne Tuytelaars. Memory aware synapses: Learning what (not) to forget. In *ECCV*, 2018.

Rahaf Aljundi, Klaas Kelchtermans, and Tinne Tuytelaars. Task-free continual learning. In *Proceedings of the IEEE/CVF conference on computer vision and pattern recognition*, pp. 11254–11263, 2019a.

Rahaf Aljundi, Min Lin, Baptiste Goujaud, and Yoshua Bengio. Gradient based sample selection for online continual learning. *Advances in neural information processing systems*, 32, 2019b.

Ali Furkan Biten, Ruben Tito, Andres Mafla, Lluis Gomez, Marçal Rusinol, Ernest Valveny, CV Jawahar, and Dimosthenis Karatzas. Scene text visual question answering. In *ICCV*, 2019.

Yaroslav Bulatov. Notmnist dataset. *Google (Books/OCR), Tech. Report*, 2, 2011.

Mathilde Caron, Ishan Misra, Julien Mairal, Priya Goyal, Piotr Bojanowski, and Armand Joulin. Unsupervised learning of visual features by contrasting cluster assignments. *Advances in neural information processing systems*, 33:9912–9924, 2020.

Mathilde Caron, Hugo Touvron, Ishan Misra, Hervé Jégou, Julien Mairal, Piotr Bojanowski, and Armand Joulin. Emerging properties in self-supervised vision transformers. In *Proceedings of the IEEE/CVF international conference on computer vision*, pp. 9650–9660, 2021.

Arslan Chaudhry, Puneet K Dokania, Thalaiyasingam Ajanthan, and Philip HS Torr. Riemannian walk for incremental learning: Understanding forgetting and intransigence. In *ECCV*, 2018.

Arslan Chaudhry, Marcus Rohrbach, Mohamed Elhoseiny, Thalaiyasingam Ajanthan, Puneet K Dokania, Philip HS Torr, and Marc'Aurelio Ranzato. On tiny episodic memories in continual learning. *arXiv preprint arXiv:1902.10486*, 2019.

Lin Chen, Jisong Li, Xiaoyi Dong, Pan Zhang, Conghui He, Jiaqi Wang, Feng Zhao, and Dahua Lin. Sharegpt4v: Improving large multi-modal models with better captions. *arXiv preprint arXiv:2311.12793*, 2023a.

Ting Chen, Saurabh Saxena, Lala Li, David J Fleet, and Geoffrey Hinton. Pix2seq: A language modeling framework for object detection. *arXiv preprint arXiv:2109.10852*, 2021.

Xi Chen, Josip Djolonga, Piotr Padlewski, Basil Mustafa, Soravit Changpinyo, Jialin Wu, Carlos Riquelme Ruiz, Sebastian Goodman, Xiao Wang, Yi Tay, et al. Pali-x: On scaling up a multilingual vision and language model. *arXiv preprint arXiv:2305.18565*, 2023b.

Xi Chen, Xiao Wang, Soravit Changpinyo, AJ Piergiovanni, Piotr Padlewski, Daniel Salz, Sebastian Goodman, Adam Grycner, Basil Mustafa, Lucas Beyer, et al. Pali: A jointly-scaled multilingual language-image model. *ICLR*, 2023c.

Yahui Chen. Convolutional neural network for sentence classification. Master's thesis, University of Waterloo, 2015.

Alexis Conneau, Douwe Kiela, Holger Schwenk, Loïc Barrault, and Antoine Bordes. Supervised learning of universal sentence representations from natural language inference data. *arXiv preprint arXiv:1705.02364*, 2017.

Jacob Devlin, Ming-Wei Chang, Kenton Lee, and Kristina Toutanova. Bert: Pre-training of deep bidirectional transformers for language understanding. *arXiv preprint arXiv:1810.04805*, 2018.

Alexey Dosovitskiy, Lucas Beyer, Alexander Kolesnikov, Dirk Weissenborn, Xiaohua Zhai, Thomas Unterthiner, Mostafa Dehghani, Matthias Minderer, Georg Heigold, Sylvain Gelly, et al. An image is worth 16x16 words: Transformers for image recognition at scale. *arXiv preprint arXiv:2010.11929*, 2020.

Saurabh Garg, Mehrdad Farajtabar, Hadi Pouransari, Raviteja Vemulapalli, Sachin Mehta, Oncel Tuzel, Vaishaal Shankar, and Fartash Faghri. Tic-clip: Continual training of clip models. *arXiv preprint arXiv:2310.16226*, 2023.

Gemini Team Google. Gemini: A family of highly capable multimodal models. *arXiv preprint arXiv:2312.11805*, 2024.

Yash Goyal, Tejas Khot, Douglas Summers-Stay, Dhruv Batra, and Devi Parikh. Making the v in vqa matter: Elevating the role of image understanding in visual question answering. In *CVPR*, 2017.

Danna Gurari, Qing Li, Abigale J Stangl, Anhong Guo, Chi Lin, Kristen Grauman, Jiebo Luo, and Jeffrey P Bigham. Vizwiz grand challenge: Answering visual questions from blind people. In *CVPR*, 2018.

Danna Gurari, Yinan Zhao, Meng Zhang, and Nilavra Bhattacharya. Captioning images taken by people who are blind. In *ECCV*, 2020.

Jinghan He, Haiyun Guo, Ming Tang, and Jinqiao Wang. Continual instruction tuning for large multimodal models. *arXiv preprint arXiv:2311.16206*, 2023.

Dan Hendrycks, Steven Basart, Norman Mu, Saurav Kadavath, Frank Wang, Evan Dorundo, Rahul Desai, Tyler Zhu, Samyak Parajuli, Mike Guo, Dawn Song, Jacob Steinhardt, and Justin Gilmer. The many faces of robustness: A critical analysis of out-of-distribution generalization. *ICCV*, 2021.

Neil Houlsby, Andrei Giurgiu, Stanislaw Jastrzebski, Bruna Morrone, Quentin De Laroussilhe, Andrea Gesmundo, Mona Attariyan, and Sylvain Gelly. Parameter-efficient transfer learning for nlp. In *International Conference on Machine Learning*, pp. 2790–2799. PMLR, 2019.

Yen-Chang Hsu, Yen-Cheng Liu, Anita Ramasamy, and Zsolt Kira. Re-evaluating continual learning scenarios: A categorization and case for strong baselines. *arXiv preprint arXiv:1810.12488*, 2018.

Edward J Hu, Yelong Shen, Phillip Wallis, Zeyuan Allen-Zhu, Yuanzhi Li, Shean Wang, Lu Wang, and Weizhu Chen. Lora: Low-rank adaptation of large language models. *arXiv preprint arXiv:2106.09685*, 2021.

Drew A Hudson and Christopher D Manning. Gqa: A new dataset for real-world visual reasoning and compositional question answering. In *CVPR*, 2019.

Ahmet Iscen, Jeffrey Zhang, Svetlana Lazebnik, and Cordelia Schmid. Memory-efficient incremental learning through feature adaptation. In *ECCV*, 2020.

Kushal Kafle and Christopher Kanan. An analysis of visual question answering algorithms. In *ICCV*, 2017.

Andrej Karpathy and Li Fei-Fei. Deep visual-semantic alignments for generating image descriptions. In *Proceedings of the IEEE conference on computer vision and pattern recognition*, pp. 3128–3137, 2015.

Sahar Kazemzadeh, Vicente Ordonez, Mark Matten, and Tamara Berg. Referitgame: Referring to objects in photographs of natural scenes. In *EMNLP*, 2014.

Zixuan Ke, Yijia Shao, Haowei Lin, Tatsuya Konishi, Gyuhak Kim, and Bing Liu. Continual pre-training of language models. *arXiv preprint arXiv:2302.03241*, 2023.

Aniruddha Kembhavi, Mike Salvato, Eric Kolve, Minjoon Seo, Hannaneh Hajishirzi, and Ali Farhadi. A diagram is worth a dozen images. In *ECCV*, 2016.

Muhammad Gul Zain Ali Khan, Muhammad Ferjad Naeem, Luc Van Gool, Didier Stricker, Federico Tombari, and Muhammad Zeshan Afzal. Introducing language guidance in prompt-based continual learning. In *CVPR*, 2023.

James Kirkpatrick, Razvan Pascanu, Neil Rabinowitz, Joel Veness, Guillaume Desjardins, Andrei A Rusu, Kieran Milan, John Quan, Tiago Ramalho, Agnieszka Grabska-Barwinska, et al. Overcoming catastrophic forgetting in neural networks. *Proceedings of the national academy of sciences*, 114 (13):3521–3526, 2017.

Alex Krizhevsky, Geoffrey Hinton, et al. Learning multiple layers of features from tiny images. *Proceedings of the IEEE*, 2009.

Yann LeCun, Léon Bottou, Yoshua Bengio, and Patrick Haffner. Gradient-based learning applied to document recognition. *Proceedings of the IEEE*, 86, 1998.

Brian Lester, Rami Al-Rfou, and Noah Constant. The power of scale for parameter-efficient prompt tuning. *arXiv preprint arXiv:2104.08691*, 2021.

Junnan Li, Dongxu Li, Caiming Xiong, and Steven Hoi. Blip: Bootstrapping language-image pre-training for unified vision-language understanding and generation. In *ICML*, 2022.

Junnan Li, Dongxu Li, Silvio Savarese, and Steven Hoi. Blip-2: Bootstrapping language-image pre-training with frozen image encoders and large language models. *arXiv preprint arXiv:2301.12597*, 2023.

Xiang Lisa Li and Percy Liang. Prefix-tuning: Optimizing continuous prompts for generation. *arXiv preprint arXiv:2101.00190*, 2021.

Zhizhong Li and Derek Hoiem. Learning without forgetting. *IEEE TPAMI*, 40, 2017.

Tsung-Yi Lin, Michael Maire, Serge J. Belongie, Lubomir D. Bourdev, Ross B. Girshick, James Hays, Pietro Perona, Deva Ramanan, Piotr Doll'a r, and C. Lawrence Zitnick. Microsoft COCO: common objects in context. *CoRR*, abs/1405.0312, 2014. URL `http://arxiv.org/abs/1405.0312`.

Haotian Liu, Chunyuan Li, Qingyang Wu, and Yong Jae Lee. Visual instruction tuning. *NeurIPS*, 2023.

Kenneth Marino, Mohammad Rastegari, Ali Farhadi, and Roozbeh Mottaghi. Ok-vqa: A visual question answering benchmark requiring external knowledge. In *CVPR*, 2019.

Ahmed Masry, Do Xuan Long, Jia Qing Tan, Shafiq Joty, and Enamul Hoque. Chartqa: A benchmark for question answering about charts with visual and logical reasoning. *arXiv preprint arXiv:2203.10244*, 2022.

Minesh Mathew, Dimosthenis Karatzas, and CV Jawahar. Docvqa: A dataset for vqa on document images. In *WACV*, 2021.

Minesh Mathew, Viraj Bagal, Rubèn Tito, Dimosthenis Karatzas, Ernest Valveny, and CV Jawahar. Infographicvqa. In *WACV*, 2022.

Michael McCloskey and Neal J Cohen. Catastrophic interference in connectionist networks: The sequential learning problem. In *Psychology of learning and motivation*, volume 24. none, 1989.

Anand Mishra, Shashank Shekhar, Ajeet Kumar Singh, and Anirban Chakraborty. Ocr-vqa: Visual question answering by reading text in images. In *ICDAR*, 2019.

Rafael Müller, Simon Kornblith, and Geoffrey E Hinton. When does label smoothing help? *NeurIPS*, 2019.

Yuval Netzer, Tao Wang, Adam Coates, Alessandro Bissacco, Bo Wu, and Andrew Y Ng. Reading digits in natural images with unsupervised feature learning. *Proceedings of the IEEE*, 2011.

Maria-Elena Nilsback and Andrew Zisserman. Automated flower classification over a large number of classes. In *Indian conference on computer vision, graphics & image processing*, 2008.

OpenAI. GPT-4 technical report. *arXiv preprint arXiv:2303.08774*, 2023.

Ameya Prabhu, Zhipeng Cai, Puneet Dokania, Philip Torr, Vladlen Koltun, and Ozan Sener. Online continual learning without the storage constraint. *arXiv preprint arXiv:2305.09253*, 2023.

Zi Qian, Xin Wang, Xuguang Duan, Pengda Qin, Yuhong Li, and Wenwu Zhu. Decouple before interact: Multi-modal prompt learning for continual visual question answering. In *ICCV*, 2023.

Alec Radford, Jong Wook Kim, Chris Hallacy, Aditya Ramesh, Gabriel Goh, Sandhini Agarwal, Girish Sastry, Amanda Askell, Pamela Mishkin, Jack Clark, Gretchen Krueger, and Ilya Sutskever. Learning transferable visual models from natural language supervision. In *ICML*, 2021.

Aditya Ramesh, Mikhail Pavlov, Gabriel Goh, Scott Gray, Chelsea Voss, Alec Radford, Mark Chen, and Ilya Sutskever. Zero-shot text-to-image generation. In *International conference on machine learning*, pp. 8821–8831. Pmlr, 2021.

Sylvestre-Alvise Rebuffi, Alexander Kolesnikov, Georg Sperl, and Christoph H Lampert. icarl: Incremental classifier and representation learning. In *CVPR*, 2017.

Andrei A Rusu, Neil C Rabinowitz, Guillaume Desjardins, Hubert Soyer, James Kirkpatrick, Koray Kavukcuoglu, Razvan Pascanu, and Raia Hadsell. Progressive neural networks. *arXiv preprint arXiv:1606.04671*, 2016.

Piyush Sharma, Nan Ding, Sebastian Goodman, and Radu Soricut. Conceptual captions: A cleaned, hypernymed, image alt-text dataset for automatic image captioning. In *Association for Computational Linguistics*, 2018.

Oleksii Sidorov, Ronghang Hu, Marcus Rohrbach, and Amanpreet Singh. Textcaps: a dataset for image captioning with reading comprehension. In *ECCV*, 2020.

Amanpreet Singh, Vivek Natarajan, Meet Shah, Yu Jiang, Xinlei Chen, Dhruv Batra, Devi Parikh, and Marcus Rohrbach. Towards vqa models that can read. In *CVPR*, 2019.

Tejas Srinivasan, Ting-Yun Chang, Leticia Pinto Alva, Georgios Chochlakis, Mohammad Rostami, and Jesse Thomason. Climb: A continual learning benchmark for vision-and-language tasks. *NeurIPS*, 2022.

Yu-Ming Tang, Yi-Xing Peng, and Wei-Shi Zheng. When prompt-based incremental learning does not meet strong pretraining. In *ICCV*, 2023.

Gido M Van de Ven and Andreas S Tolias. Three scenarios for continual learning. *arXiv preprint arXiv:1904.07734*, 2019.

Aaron Van Den Oord, Oriol Vinyals, et al. Neural discrete representation learning. *Advances in neural information processing systems*, 30, 2017.

Bryan Wang, Gang Li, Xin Zhou, Zhourong Chen, Tovi Grossman, and Yang Li. Screen2words: Automatic mobile ui summarization with multimodal learning. In *The 34th Annual ACM Symposium on User Interface Software and Technology*, 2021.

Jianfeng Wang, Zhengyuan Yang, Xiaowei Hu, Linjie Li, Kevin Lin, Zhe Gan, Zicheng Liu, Ce Liu, and Lijuan Wang. Git: A generative image-to-text transformer for vision and language. *arXiv preprint arXiv:2205.14100*, 2022a.

Yu-Xiong Wang, Deva Ramanan, and Martial Hebert. Growing a brain: Fine-tuning by increasing model capacity. In *CVPR*, 2017.

Zifeng Wang, Zizhao Zhang, Sayna Ebrahimi, Ruoxi Sun, Han Zhang, Chen-Yu Lee, Xiaoqi Ren, Guolong Su, Vincent Perot, Jennifer Dy, et al. Dualprompt: Complementary prompting for rehearsal-free continual learning. In *ECCV*, 2022b.

Zifeng Wang, Zizhao Zhang, Chen-Yu Lee, Han Zhang, Ruoxi Sun, Xiaoqi Ren, Guolong Su, Vincent Perot, Jennifer Dy, and Tomas Pfister. Learning to prompt for continual learning. In *CVPR*, 2022c.

Han Xiao, Kashif Rasul, and Roland Vollgraf. Fashion-mnist: a novel image dataset for benchmarking machine learning algorithms. *arXiv preprint arXiv:1708.07747*, 2017.

Shipeng Yan, Jiangwei Xie, and Xuming He. Der: Dynamically expandable representation for class incremental learning. In *CVPR*, 2021.

Peter Young, Alice Lai, Micah Hodosh, and Julia Hockenmaier. From image descriptions to visual denotations: New similarity metrics for semantic inference over event descriptions. *Transactions of the Association for Computational Linguistics*, 2, 2014.

Xi Zhang, Feifei Zhang, and Changsheng Xu. Vqacl: A novel visual question answering continual learning setting. In *CVPR*, 2023.

Zangwei Zheng, Mingyuan Ma, Kai Wang, Ziheng Qin, Xiangyu Yue, and Yang You. Preventing zero-shot transfer degradation in continual learning of vision-language models. *arXiv preprint arXiv:2303.06628*, 2023.

Table 7: **Statistics for 36 datasets and 8 applications**.

Dataset	Visual Domain	#Train	#Val	#Test	Metric
Captioning					
COCO Lin et al. (2014)	Natural Images	113287	5000	5000	CIDEr
Flickr30K Young et al. (2014)	Natural Images	29000	1014	1000	
TextCaps Sidorov et al. (2020) (**w/o OCR**)	Natural Images	109725	15830	-	
VizWiz-Cap Gurari et al. (2018) (**w/o OCR**)	Natural Images	100575	33145	-	
Screen2Words Wang et al. (2021) (**w/o OCR**)	UIs	15743	2364	4310	
BLIP-LCS Li et al. (2022); Liu et al. (2023)	Natural Images	446502	111626	-	
ShareGPT4V-PT Chen et al. (2023a)	Natural Images	997520	249381	-	
VQA					
VQAv2 Goyal et al. (2017)	Natural Images	594917	26261	25829	VQA Acc.
OK-VQA Marino et al. (2019)	Natural Images	8998	5033	-	VQA Acc.
VizWiz-QA Gurari et al. (2018) (**w/o OCR**)	Natural Images	20523	4319	-	VQA Acc.
TextVQA Singh et al. (2019) (**w/o OCR**)	Natural Images	34602	5000	-	VQA Acc.
ST-VQA Biten et al. (2019) (**w/o OCR**)	Natural Images	23446	2628	-	VQA Acc.
GQA Hudson & Manning (2019)	Natural Images	943000	132062	12578	VQA Acc.
TDIUC Kafle & Kanan (2017)	Natural Images	1003061	50000	-	VQA Acc.
TallyQA Acharya et al. (2019)	Natural Images	249318	38589	-	EM
OCR-CV					
TextCaps Sidorov et al. (2020)	Natural Images	109725	15830	-	CIDEr
VizWiz-QA Gurari et al. (2020)	Natural Images	20523	4319	-	VQA Acc.
OCR-VQA Mishra et al. (2019)	Illustrations	805110	31000	31000	EM
ChartQA Masry et al. (2022)	Illustrations	28299	1920	2500	RA
DocVQA Mathew et al. (2021)	Documents	39463	5349	5188	ANLS
Screen2Words Wang et al. (2021)	UIs	15743	2364	4310	CIDEr
TextVQA Singh et al. (2019)	Natural Images	34602	5000	-	VQA Acc.
AI2D Kembhavi et al. (2016)	Illustrations	12293	120	3088	EM
InfographicsVQA Mathew et al. (2022)	Documents	23946	2801	3288	ANLS
Open-Vocabulary Classification					
CIFAR10 Krizhevsky et al. (2009)	Natural Images	50000	10000	-	EM
MNIST LeCun et al. (1998)	Natural Images	60000	10000	-	
Fashion-MNIST Xiao et al. (2017)	Natural Images	60000	10000	-	
SVHN Netzer et al. (2011)	Natural Images	73257	26032	-	
notMNIST Bulatov (2011)	Natural Images	59916	14979	-	
CIFAR100 Krizhevsky et al. (2009)	Natural Images	50000	10000	-	
ImageNet-R Hendrycks et al. (2021)	Natural Images	24000	6000	-	
Flowers Nilsback & Zisserman (2008)	Natural Images	1020	1020	-	
Detection					
COCO Lin et al. (2014)	Natural Images	113287	5000	5000	AP
Referring Expression Generation					
RefCOCO Kazemzadeh et al. (2014)	Natural Images	287604	26488	30969	CIDEr
Grounding					
RefCOCO Kazemzadeh et al. (2014)	Natural Images	287604	26488	30969	IoU
Multi-Modal Instructions					
LLaVA-158K Liu et al. (2023)	Natural Images	126169	31523	-	CIDEr

A Implementation Details

A.1 Applications

In this section, we detail the definition considered 8 applications and a total of 36 datasets we curated. See Tab. 7 for the statistics and full details.

Table 8: **Instruction template for 8 applications**.

Captioning
Generate the caption for this image.
Generate the caption
Generate the alt_text:
Describe the image.
Caption this image.
A photo of
Caption
A short image caption
summarize the given photo
detail everything you see in this image
Provide a detailed description of this image, including objects, actions, and context.
What is going on in the image?
what is the main content of this image?
what is shown in the photo
Briefly describe the content of the image.
Use a few words to illustrate what is happening in the picture.
VQA
{Question}
OCR-CV
{*Captioning* or *VQA* Instruction} + <OCR text: ...>
Open-Vocabulary Classification
Identify the primary subject in this image.
Name the object in the image.
Classify this image
classify
What do you see here?
What category does this image belong to?
What is the main object of this image?
What is shown in the photo?
what is inside this image?
what's in this picture
Detection
detect:
Referring Expression Generation
describe the box at {Location}:
Grounding
detect {Referring Expression}:
Multi-Modal Instructions
{Instruction}

Captioning requires the model to provide a concise description of visual content. The following datasets with short captions are considered: COCO Captions Lin et al. (2014) with the split defined in Karpathy & Fei-Fei (2015), Flickr30K Young et al. (2014), TextCaps Sidorov et al. (2020), VizWiz-Cap Gurari et al. (2020), Screen2Words Wang et al. (2021), and BLIP-LCS Li et al. (2022). To account for the increasing length and quality of captions generated by multi-modal instruction-following models, the ShareGPT4V-PT Chen et al. (2023a) dataset is also included, which features significantly longer and more descriptive captions.

Visual Question Answering (VQA) aims at generating textual answers based on both a textual question and visual context. For our benchmark, we use datasets where the visual context consists of natural images Chen et al. (2023b): VQAv2 Goyal et al. (2017), OKVQA Marino et al. (2019), TextVQA Singh et al. (2019), VizWiz-QA Gurari et al. (2018), ST-VQA Biten et al. (2019), GQA Hudson & Manning (2019), TDIUC Kafle & Kanan (2017), and TallyQA Acharya et al. (2019).

OCR-enhanced captioning and VQA (OCR-CV) leverage the output of an upstream OCR model to solve captioning and VQA applications. We consider the following datasets: TextCaps Sidorov et al. (2020), Screen2Words Wang et al. (2021), VizWiz-QAGurari et al. (2018), OCR-VQA Mishra et al. (2019), ChartQA Masry et al. (2022), DocVQA Mathew et al. (2021), TextVQA Singh et al. (2019), AI2D Kembhavi et al. (2016) and InfographicsVQA Mathew et al. (2022). In these datasets, OCR text tokens are extracted by an upstream OCR system Chen et al. (2023b) and provided as additional text inputs.

Open-vocabulary classification categorizes object-centric images into their corresponding classes. In our benchmark, we redefine classification as a generative task. Instead of training a set of classifier weights Chaudhry et al. (2019); Wang et al. (2022c), we use a generative model with open-world vocabulary to directly generate class names Wang et al. (2022a). The considered datasets are CIFAR10 Krizhevsky et al. (2009), CIFAR100 Krizhevsky et al. (2009), MNIST LeCun et al. (1998), notMNIST Bulatov (2011), FashionMNIST Xiao et al. (2017), SVHN Netzer et al. (2011), ImageNet-R Wang et al. (2022b), and Flowers Nilsback & Zisserman (2008).

Spatial recognition assesses the model's ability to comprehend and generate output based on spatial coordinates of the image, typically represented as bounding boxes. Following the approach of Pix2Seq Chen et al. (2021; 2023c;b), we directly incorporate discretized bounding boxes into the text input by concatenating them with the relevant object or concept. We evaluate the model for three distinct applications: i) Detection, where the bounding boxes for *all* objects are regarded as the target $\mathcal{Y}$, ii) Referring Expression Generation, where the bounding box for a *specific* object is included in the instruction $\mathcal{I}$, iii) Grounding, where the bounding box for a *specific* object is present in target $\mathcal{Y}$. All three of these applications are performed on the COCO Lin et al. (2014) dataset.

Multi-modal instruction tuning considers more complex textual $\mathcal{I}$ inputs, including but not limited to conversational-style QA, detailed descriptions, and complex reasoning. They can be seen as a super-set of all previously considered applications. For this purpose, we employ the 158K supervised fine-tuning dataset from LLaVA Liu et al. (2023) derived from COCO Lin et al. (2014) dataset.

A.2 Datasets

Here we specify the details of 36 datasets used in our experiments. Unless specified otherwise as below, we use default train and validation sets.

BLIP-LCS Li et al. (2022) & ShareGPT4V-PT Chen et al. (2023a). We use 80% of the original data as the training set and the rest of 20% as the validation set.

TDIUC Kafle & Kanan (2017). We use 10% of the original validation set as the validation set here.

OCR-VQA Mishra et al. (2019). We use 15% of the original validation set as the validation set here and another 15% as the test set.

RefCOCO Kazemzadeh et al. (2014). We count the object numbers since the evaluation is instance-wise for referring expression generation and grounding.

LLaVA-158K Liu et al. (2023). We use 158K unique language-image instruction-following samples that collected in LLaVA Liu et al. (2023). The instructions are much more diverse comparing with ones from other applications, including conversation, detailed captioning, and complex reasoning. The images are sampled from COCO Lin et al. (2014) and the answers are taken via interacting with language-only GPT-4. We use 80% of the original data as the training set and the rest of 20% as the validation set.

A.3 Pre-Processing

In this section, we detail necessary pre-processing steps for reproduction purposes. By default, we resize the image with a ratio uniformly sampled from $[0.75, 1.25]$ and pad the image's shorter side. See Tab. 8 for the instruction template we use for different applications. We tokenize the textual instructions and targets using a BERT tokenizer Devlin et al. (2018) with a vocabulary size of 30522.

Captioning. We manually append an instruction randomly sampled from a pool detailed in Tab. 8. We directly use the image caption as the target. For datasets with multiple captions (*e.g.*, COCO Captions Lin et al. (2014)), we randomly sample one.

VQA. We directly use the question as the instruction and the answer as the target from the original dataset without any other extra processing. For datasets with multiple captions (*e.g.*, VQAv2 Goyal et al. (2017)), we randomly sample one.

OCR-CV. For visual input, we do not scale the image while resizing to make sure the entire image is visible to the model. We follow the pre-processing steps as Chen et al. (2023b) using an upstream OCR system, GCP Vision API, to extract the potential OCR texts in the image. The extracted OCR texts are then appended in the format of "*<OCR text: ...>*" after the original captioning or VQA instructions.

Open-vocabulary classification. We manually append an instruction randomly sampled from a pool detailed in Tab. 8. For the target, we directly use the class label name if the mapping exists. We use "*digit {Class Label}*" for MNIST LeCun et al. (1998) and SVHN Netzer et al. (2011), "*letter {Class Label}*" for notMNIST Bulatov (2011).

Detection. For visual input, we resize the image with a ratio uniformly sampled from $[0.3, 2.0]$ and randomly flip the image. We simply use "*detect:*" as the instruction. For the target, we rescale the range of original bounding boxes in COCO Lin et al. (2014) from 1.0 to 999 (int) and concatenate 4 coordinates directly with the instance label. Different instances are directly concatenated with "*and*". An exemplar target looks like "*10 99 323 675 cat and 127 346 894 997 dog*". We do not use the augmentation trick proposed in Chen et al. (2021).

Referring expression generation. The pre-processing for visual input follows the detection task. For each instance, we use "describe the box at *{*Location}:" as the instruction and its referring expression as the target.

Grounding. The pre-processing for visual input follows the detection task. For each instance, we use "detect *{*Referring Expression}:" as the instruction and its location as the target. The formatting of the bounding boxes follows the detection task.

Multi-modal instruction tuning. We directly use human instructions as the instruction and the GPT-4 OpenAI (2023)'s output as the target.

Table 9: **Dataset-incremental learning for captioning and VQA** with different task order shuffling seed.

Seed	1		2		3		4		5		Mean		Variance	
	F↓	Score↑	F↓	Score↑	F↓	Score↑	F↓	Score↑	F↓	Score↑	F↓	Score↑	F	Score
captioning	0.47	100.8	0.04	99.8	0.32	100.6	0.59	96.2	0.09	96.1	**0.30**	**98.7**	**0.04**	**4.44**
VQA	0.54	55.1	0.77	54.9	54.9	0.03	54.8	0.71	54.4	0.09	**0.43**	**54.8**	**0.10**	**0.05**

Table 10: **Dataset-incremental learning for the captioning application.** Detailed results on each dataset for single-tasking (ST), multi-tasking (MT) and sequential tasks (Seq) are reported. All results are without OCR in the instruction.

Dataset	ST				MT		Seq						
	Fine-tuning		Adapter		Fine-tuning	Adapter	Fine-tuning	Adapter	E-Replay	L2P+	TCIA^{P}	TCIA^{Pr}	TCIA^{A}
	Val	Test	Val	Test	Val	Val	Val	Val	Val	Val	Val	Val	Val
COCO	139.8	141.7	134.2	136.1	135.6	131.3	102.1	104.7	108.0	121.4	125.9	118.6	126.1
Flickr30K	102.6	100.9	97.8	98.0	102.4	93.9	97.5	95.0	96.4	92.5	92.1	87.6	91.2
TextCaps	100.9	-	93.4	-	105.9	88.7	61.3	57.0	74.1	85.0	84.8	80.3	86.8
VizWiz-Cap	101..7	-	92.5	-	101.3	91.6	57.3	58.9	71.2	84.5	84.0	81.9	88.0
Screen2Words	85.3	84.8	78.1	79.3	70.9	62.8	46.3	29.1	66.0	61.5	60.6	70.6	73.2
BLIP-LCS	133.8	-	122.6	-	136.4	117.8	71.4	58.1	94.9	108.8	108.7	104.8	120.9
ShareGPT4V-PT	185.8	-	114.6	-	138.2	92.3	0.0	0.0	30.2	28.4	0.0	73.0	119.1
Avg	**121.4**	-	**104.7**	-	**112.9**	**96.9**	**62.3**	**57.5**	**77.3**	**83.2**	**79.4**	**88.1**	**100.8**

A.4 Metrics

For task t sampled from task mixture $\mathbf{T}$, let $\mathcal{A}_{t,i}$ be the evaluation result under task t's metric after training task i for any $i \geq t$. We report the average correctness *score* after all the tasks are trained:

$$\text{Score} = \frac{1}{T}\sum_{i}\mathcal{A}_{i,T}. \tag{1}$$

The *forgetting* metric Chaudhry et al. (2018) (denoted by F in our experiments) is computed as

$$F = \frac{1}{T}\sum_{i}\max(\mathcal{A}_{i,\geq i}) - \mathcal{A}_{i,T} \tag{2}$$

where $\max(\mathcal{A}_{i,\geq i})$ is the peak evaluation result for task i after when it is trained.

Application-Incremental Learning. To equalize the importance of each application, we first average the evaluation results across datasets within each application and then average the results across applications.

A.5 Task Order

For all experiments conducted with sequential tasks $\mathbf{T}$, we shuffle it with a fixed seed 1, *i.e.*, `import random; random.Random(1).shuffle(T)`. We include results with seeds $2, 3, 4, 5$ for captioning and VQA in Tab. 9. We report the results of dataset-incremental learning for captioning and VQA on 5 different shuffling seeds. Even though the task order is an important parameter because of the similarity between different tasks, the result indicates that our method is robust to different task orders.

B Additional Results

B.1 Dataset-Incremental Learning.

We detail the evaluation results for dataset-incremental learning on captioning, VQA, OCR-CV, and open-vocabulary classification in Tab 10, Tab. 11, Tab. 12 and Tab. 13, respectively. Results on

Table 11: **Dataset-incremental learning for the VQA application.** Detailed results on each dataset for single-tasking (ST), multi-tasking (MT) and sequential tasks (Seq) are reported. All results are without OCR in the instruction.

Dataset	ST				MT		Seq						
	Fine-tuning		Adapter		Fine-tuning	Adapter	Fine-tuning	Adapter	E-Replay	L2P	TCIA$^{\mathrm{P}}$	TCIA$^{\mathrm{Pr}}$	TCIA$^{\mathrm{A}}$
	Val	Test	Val	Test	Val	Val	Val	Val	Val	Val	Val	Val	Val
VQAv2	75.1	74.6	74.6	74.5	74.8	72.1	62.4	55.1	72.1	51.2	65.5	69.8	72.8
OK-VQA	38.1	-	41.9	-	49.2	47.7	22.8	15.5	35.3	35.8	34.3	39.7	40.4
VizWiz-QA	56.9	-	56.3	-	57.6	55.3	56.5	55.2	54.3	52.9	53.3	53.5	56.4
TextVQA	32.6	-	30.7	-	33.9	30.3	21.5	20.0	22.4	26.6	25.7	28.5	29.8
ST-VQA	27.6	-	25.9	-	31.6	27.2	21.3	17.9	23.8	21.3	20.6	22.3	24.6
GQA	66.7	57.9	63.6	56.2	67.3	63.6	46.9	36.7	61.7	59.2	54.5	56.3	59.1
TDIUC	91.2	-	91.0	-	92.7	90.9	60.4	53.4	90.6	80.3	89.1	90.4	90.8
TallyQA	65.6	-	67.0	-	67.7	67.3	47.5	37.4	61.8	64.0	63.2	65.1	66.7
Avg	**56.7**	-	**56.4**	-	**59.4**	**56.8**	**42.4**	**36.4**	**52.7**	**48.9**	**50.7**	**53.2**	**55.1**

Table 12: **Dataset-incremental learning for the OCR-CV application.** Detailed results on each dataset for single-tasking (ST), multi-tasking (MT) and sequential tasks (Seq) are reported. All results are with OCR in the instruction.

Dataset	ST				MT		Seq						
	Fine-tuning		Adapter		Fine-tuning	Adapter	Fine-tuning	Adapter	E-Replay	L2P+	TCIA$^{\mathrm{P}}$	TCIA$^{\mathrm{Pr}}$	TCIA$^{\mathrm{A}}$
	Val	Test	Val	Test	Val	Val	Val	Val	Val	Val	Val	Val	Val
TextCaps	101.0	-	99.8	-	104.7	88.9	13.0	5.1	83.5	81.5	81.9	80.7	95.7
VizWiz-QA	56.9	-	55.8	-	57.1	53.0	16.0	7.0	42.9	52.3	51.1	53.3	56.4
OCR-VQA	70.1	70.3	62.6	63.0	61.5	56.8	61.0	58.2	61.0	48.0	46.6	51.5	60.3
ChartQA	18.3	17.4	19.8	19.5	19.2	18.4	10.7	3.1	12.9	12.7	12.6	14.3	18.9
DocVQA	16.4	4.2	20.3	6.6	7.2	4.2	1.9	1.0	3.7	4.5	3.2	9.1	14.5
Screen2Words	98.0	97.6	91.9	95.5	29.9	34.6	8.4	3.8	23.1	67.5	67.5	74.6	85.6
TextVQA	36.7	-	34.5	-	41.5	38.3	18.0	7.7	27.2	17.1	26.2	29.6	35.3
AI2D	35.0	30.6	40.0	35.3	37.5	40.0	3.3	0.8	15.8	28.3	24.2	31.7	37.5
InfographicsVQA	9.4	4.0	11.1	6.6	4.8	2.0	0.6	0.0	2.3	6.6	4.3	7.6	6.9
Avg	**49.1**	-	**48.4**	-	**40.4**	**37.4**	**14.8**	**9.6**	**30.3**	**35.4**	**35.3**	**39.2**	**45.7**

Table 13: **Dataset-incremental learning for the open-vocabulary classification application.** Detailed results on each dataset for single-tasking (ST), multi-tasking (MT) and sequential tasks (Seq) are reported.

Dataset	ST				MT		Seq						
	Fine-tuning		Adapter		Fine-tuning	Adapter	Fine-tuning	Adapter	E-Replay	L2P+	TCIA$^{\mathrm{P}}$	TCIA$^{\mathrm{Pr}}$	TCIA$^{\mathrm{A}}$
	Val	Test	Val	Test	Val	Val	Val	Val	Val	Val	Val	Val	Val
CIFAR10	99.4	-	98.6	-	98.7	96.9	73.7	2.2	95.8	97.4	97.6	97.8	98.3
MNIST	99.3	-	99.4	-	99.7	99.3	0.0	0.0	97.5	98.8	98.7	99.0	99.2
Fashion-MNIST	96.2	-	94.0	-	96.2	93.5	95.9	93.2	95.8	90.9	91.2	91.5	93.4
SVHN	98.0	-	90.8	-	98.1	89.2	0.0	0.0	88.2	81.6	81.5	84.8	89.3
notMNIST	97.9	-	95.9	-	97.8	95.1	0.0	0.0	62.4	92.6	92.4	93.7	95.1
CIFAR100	94.1	-	89.6	-	93.1	87.6	18.3	0.1	50.7	82.7	85.3	86.4	88.0
ImageNet-R	93.5	-	93.3	-	93.5	92.7	3.0	0.2	19.3	90.7	90.6	92.1	92.9
Flowers	98.0	-	96.3	-	98.2	96.2	2.2	0.0	26.5	91.9	91.2	94.7	95.9
Avg	**97.1**	-	**94.7**	-	**96.9**	**93.8**	**24.2**	**11.9**	**67.0**	**90.8**	**90.9**	**92.5**	**94.0**

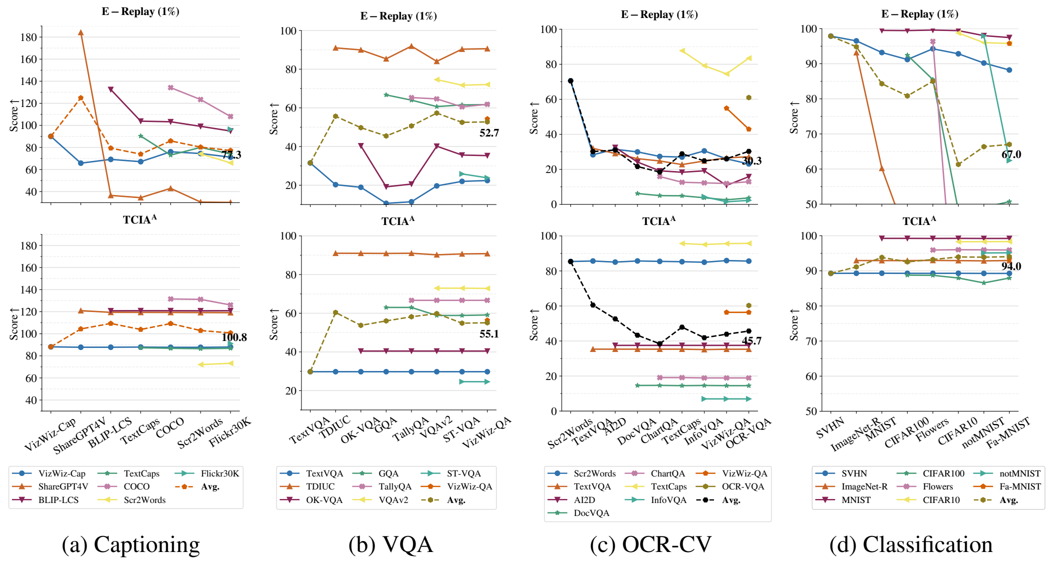

Figure 6: **Dataset-incremental learning** with incremental learning scores over training steps. We compare TCIA$^{\mathrm{A}}$ (**bottom**) to the E-Replay Chaudhry et al. (2019) method (**top**) with buffer size being 1% of the entire training data. TCIA$^{\mathrm{A}}$ exhibits minimal forgetting, hence better final accuracy (*Avg.*).

Table 14: **Instruction-incremental learning.** Detailed results on each dataset for single-tasking (ST), multi-tasking (MT), and sequential tasks (Seq) are reported.

Dataset	ST		MT		Seq			Metrics
	Fine-tuning	Adapter	Fine-tuning	Adapter	E-Replay	L2P+	TCIA$^{\mathrm{A}}$	
	Val	Val	Val	Val	Val	Val	Val	
Captioning								
COCO	139.8	134.2	132.8	130.5	114.2	132.3	130.2	CIDEr
VQA								
OK-VQA	38.1	41.9	38.9	41.2	35.0	38.1	39.8	VQA Acc.
Detection								
COCO	20.1	4.3	12.9	2.80	11.2	0.7	3.3	AP
Referring Expression Generation								
RefCOCO	92.7	76.8	86.1	89.0	62.9	63.0	85.0	CIDEr
Grounding								
RefCOCO	66.1	44.7	61.8	47.0	46.0	21.1	44.8	IoU
Avg	**71.4**	**60.4**	**66.8**	**62.1**	**53.9**	**51.1**	**60.6**	Score

detection, referring expression generation, and grounding are with an image resolution of 352, which is chosen as the multiple of 32 closest to 336. All the other results are with an image resolution of 224. The 4 dataset-incremental learning settings on captioning, VQA, OCR-CV, and open-vocabulary classification are trained with 60K, 60K, 45K, and 20K iterations, respectively. The training is conducted with TPU v4 chips.

Incremental learning score curve. Additionally, we visualize the incremental learning scores over training steps in Fig. 6. We see that the performance curves of TCIA$^{\mathrm{A}}$ stay flat as training proceeds, while those of the E-Replay method undergo a noticeable drop, indicating catastrophic forgetting.

Table 15: **Class-incremental learning on varying class splits of CIFAR100 Krizhevsky et al. (2009); Wang et al. (2022c).** *Rep.* denotes the task key representation we use to learn task-specific keys. We specify the type of head used to perform classification: *Classes* refer to a standard unfrozen linear classification head. *Text Vocabulary* is a frozen linear layer outputting word tokens logits. In this case, classification is performed by auto-regressively generating the class label name. All the numbers are run by us.

Method	Model	Rep.	Head	5 splits		10 splits		20 splits		100 splits	
				F↓	Score ↑	F↓	Score ↑	F↓	Score ↑	F↓	Score ↑
Upper-bound	ViT-B	–	Classes	–	90.9	–	90.9	–	90.9	–	90.9
Upper-bound	GiT-L	–	Classes	–	94.1	–	94.1	–	94.1	–	94.1
L2P	ViT-B	ViT-B	Classes	87.9	24.0	7.82	83.1	10.4	80.6	84.5	3.82
E-Replay	GIT-L	–	Classes	5.37	85.3	**6.12**	83.9	7.44	82.8	76.2	20.4
TCIA	GIT-L	max-pooling	Classes	4.60	86.5	6.41	**87.6**	7.34	83.1	4.50	11.2
TCIA	GIT-L	max-pooling	Text Vocabulary	6.18	84.3	10.2	81.7	4.11	88.0	1.42	97.0
TCIA	GIT-L	CLIP-B	Text Vocabulary	**2.32**	86.4	11.0	83.4	4.73	87.2	0.87	96.7
TCIA	GIT-L	ViT-B	Text Vocabulary	2.54	**90.3**	9.16	87.0	**2.18**	**94.3**	**0.75**	**98.1**

B.2 Class-Incremental Learning.

Class-incremental learning with varying splits on CIFAR100. Here, we explore different ways of splitting CIFAR100 for class-incremental learning. We vary the number of splits from 5 to 100 and report results in Tab. 15. Note that having more splits results in a lower number of classes per split, which makes incremental learning more challenging. In fact, with 100 splits, there is only one class per task. Note that this scenario may not be deemed very practical, but we use it to investigate the performance of our method in an extreme setting.

We observe in Tab. 15 that TCIA is robust to the number of considered splits. Both L2P Wang et al. (2022c) and E-Replay Chaudhry et al. (2019) fail when trained incrementally class per class (*i.e.* 100 splits). We find that this is mainly because these baselines use a standard *unfrozen* classification head, which cannot be trained properly by seeing only one class at a time. In contrast, because we build on a generative image-to-text model, we perform classification by auto-regressively generating class names. This way, our default setting is to use a *frozen* text vocabulary classifier as the final head, which outputs logits for word tokens. This alleviates the issue of having to learn a single classification head vector at a time and explains why TCIA obtains a good performance in the 100 splits setting. In fact, we get poor performance similar to L2P and E-Replay when using a classification head instead of a vocabulary head in the TCIA framework. Finally, we see in Tab. 15 that building task-specific keys from additional models CLIP-B Radford et al. (2021) or ViT-B Dosovitskiy et al. (2020) works better than our default design of using inner GiT-L decoder features. Overall, our analysis in Tab. 15 shows the benefit of leveraging generative auto-regressive models for extreme class-incremental learning such as learning one class at a time.

Accuracy score. We visualize the incremental learning scores of E-Replay and TCIA across the training steps in Fig. 7.

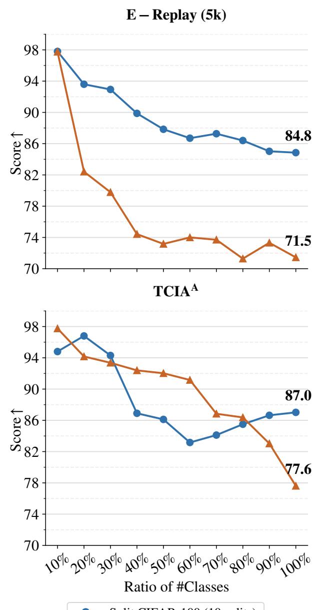

B.3 Instruction-Incremental Learning.

We detail the evaluation results for instruction-incremental learning from Tab. 4 in Tab. 14. Results are with an image resolution of 352 with 60K iterations. The training is conducted with TPU v4 chips.

B.4 Application-Incremental Learning.

We detail the evaluation results for application-incremental learning from Tab. 5 in in Tab. 16. Results are with an image resolution of 352 with 400K iterations. The training is conducted with TPU v4 chips.

Table 16: **Application-incremental learning.** Detailed results on each dataset for multi-tasking (MT) and sequential tasks (Seq) are reported. For sequential tasks, two setup on 8 applications (*App.*) and 36 datasets (*Data.*) are reported.

Dataset	MT		Seq (8 App.)			Seq (36 Data.)			Metrics
	Fine-tuning	Adapter	E-Replay	L2P+	TCIA^{A}	E-Replay	L2P+	TCIA^{A}	
	Val	Val	Val	Val	Val	Val	Val	Val	
Captioning									
COCO	121.3	118.0	103.5	90.5	27.1	95.3	42.2	119.3	
Flickr30K	79.0	89.9	63.8	80.3	26.7	54.8	63.9	85.1	
TextCaps (**w/o OCR**)	102.5	80.1	90.8	62.0	55.7	73.3	52.3	76.3	
VizWiz-Cap (**w/o OCR**)	93.2	78.4	67.1	21.6	53.3	63.7	57.2	79.4	CIDEr
Screen2Words (**w/o OCR**)	36.7	29.6	25.7	17.0	19.6	37.6	11.1	65.2	
BLIP-LCS	124.4	96.6	77.5	88.8	103.0	69.4	93.1	105.2	
ShareGPT4V-PT	156.7	106.7	89.9	71.6	137.4	50.4	75.5	138.6	
VQA									
VQAv2	73.0	69.2	65.3	62.9	71.0	70.4	47.9	67.9	
OK-VQA	46.2	45.1	31.2	21.9	43.1	44.1	29.4	40.4	
VizWiz-QA (**w/o OCR**)	54.5	48.7	50.7	20.8	40.2	43.4	44.24	51.6	
TextVQA (**w/o OCR**)	47.3	30.9	41.5	22.9	29.4	31.8	24.6	29.4	VQA Acc.
ST-VQA (**w/o OCR**)	42.2	27.5	35.1	19.4	26.7	27.7	20.5	24.7	
GQA	63.9	63.2	54.7	57.2	63.6	59.1	42.4	58.1	
TDIUC	46.2	90.2	88.6	88.0	90.6	88.9	86.3	88.8	
TallyQA	54.5	67.1	59.5	61.1	68.2	61.3	65.3	64.4	EM
OCR-CV									
TextCaps	47.3	96.2	100.2	40.5	95.6	75.7	54.8	85.5	CIDEr
VizWiz-QA	42.2	49.9	51.6	14.5	47.0	45.5	46.6	53.3	VQA Acc.
OCR-VQA	63.9	55.9	58.4	43.0	58.7	47.5	46.5	59.5	EM
ChartQA	91.1	21.5	26.1	12.4	25.9	14.4	14.0	20.0	RA
DocVQA	66.5	22.3	8.9	27.9	26.5	11.1	9.1	19.1	ANLS
Screen2Words	105.3	31.7	26.9	20.5	39.3	39.4	6.5	71.6	CIDEr
TextVQA	54.9	40.7	48.1	21.2	42.3	34.0	23.8	33.6	VQA Acc.
AI2D	40.8	35.0	42.5	2.5	36.7	8.3	24.2	35.0	EM
InfographicsVQA	12.8	10.4	11.3	5.6	10.5	6.0	3.4	6.9	ANLS
Open-Vocabulary Classification									
CIFAR10	98.3	94.5	90.2	94.0	94.5	97.4	17.9	96.9	
MNIST	99.7	99.1	98.3	98.5	99.3	99.4	99.2	99.2	
Fashion-MNIST	96.1	92.4	89.3	90.1	93.2	92.0	90.2	93.4	
SVHN	97.9	88.3	92.0	82.6	89.5	93.8	85.5	91.0	EM
notMNIST	98.1	94.4	95.0	92.3	94.8	91.9	89.2	95.2	
CIFAR100	91.7	82.4	59.8	78.9	83.1	64.0	75.5	83.8	
ImageNet-R	90.5	90.3	37.6	85.1	55.8	36.2	86.8	91.6	
Flowers	98.0	94.5	28.5	87.4	95.4	24.6	87.5	96.1	
Detection									
COCO	14.1	1.2	8.9	0.3	3.2	10.9	0.3	3.5	AP
Referring Expression Generation									
RefCOCO	97.6	73.7	55.3	60.4	74.7	61.4	67.1	81.2	CIDEr
Grounding									
RefCOCO	65.9	31.3	41.8	20.1	47.0	50.8	20.8	47.1	IoU
Multi-Modal Instructions									
LLaVA-158K	59.3	46.8	43.9	30.4	61.8	65.1	30.8	61.9	CIDEr
Avg	**72.7**	**63.7**	**57.7**	**49.3**	**59.2**	**53.9**	**48.2**	**67.2**	Score

Table 17: **Ablation study** on different choices of sequence representation and task codebook depth l with task codebook lookup accuracy (Acc_L). Task key representations including (a) `[CLS]`; (b) `[EOS]`; (c) `[[CLS];[EOS]]`; (d) mean-pooling; (e) max-pooling; (f) `[[CLS];max-pooling]`; (g) `[[CLS];[EOS];max-pooling]` (h) CLIP-B Radford et al. (2021) are ablated. The default setup is underlined.

l	(a)	(b)	(c)	(d)	(e)	(f)	(g)	(h)
0	89.2	28.2	93.4	89.2	96.1	91.0	92.8	85.3
1	88.7	36.4	89.4	90.6	94.1	92.0	93.9	85.3
2	88.4	66.9	89.6	92.2	93.9	92.2	93.4	85.3
3	90.3	53.8	88.4	92.7	87.1	92.7	91.2	85.3

(i) Dataset-incremental learning on captioning datasets.

l	(a)	(b)	(c)	(d)	(e)	(f)	(g)	(h)
0	89.5	23.8	89.5	89.9	99.4	99.8	99.7	88.1
1	89.9	48.9	90.7	94.3	98.8	99.3	97.4	88.1
2	94.2	76.9	94.5	93.1	98.0	93.8	97.1	88.1
3	95.2	84.6	95.5	93.7	96.7	89.7	92.3	88.1

(ii) Dataset-incremental learning on OCR-CV datasets.

l	(a)	(b)	(c)	(d)	(e)	(f)	(g)	(h)
0	99.5	12.4	97.3	99.9	99.9	99.9	98.4	99.7
1	99.5	17.0	97.6	99.9	93.8	99.8	97.6	99.7
2	98.4	55.4	99.1	99.9	95.3	99.7	99.4	99.7
3	98.2	61.7	95.9	99.9	95.8	99.7	99.4	99.7

(iii) Dataset-incremental learning on classification datasets.

l	(a)	(b)	(c)	(d)	(e)	(f)	(g)	(h)
0	42.5	10.6	42.4	72.8	84.0	54.7	56.3	84.7
1	40.7	16.7	39.6	73.1	65.8	54.7	57.1	84.7
2	42.5	14.0	45.9	78.9	60.5	57.6	60.1	84.7
3	46.3	11.0	42.2	82.7	71.5	56.6	53.6	84.7

(iv) Class-incremental learning on 10 splits of the CIFAR100 Krizhevsky et al. (2009) dataset.

l	(a)	(b)	(c)	(d)	(e)	(f)	(g)	(h)
0	25.5	99.9	99.9	47.0	100	95.4	100	100
1	27.7	99.7	99.9	50.4	99.9	90.7	100	100
2	57.6	99.9	100	76.2	98.1	94.9	99.9	100
3	86.5	100	99.9	78.9	93.2	98.4	99.9	100

(v) Instruction-incremental learning on the COCO Lin et al. (2014) dataset.

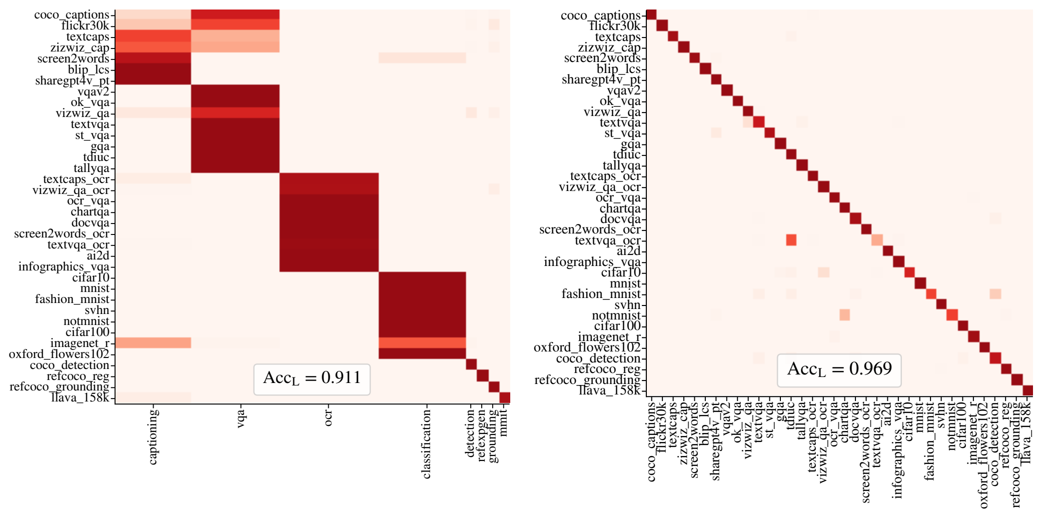

Figure 8: **Confusion matrix** for application-incremental learning across 8 applications (left) and 36 datasets (right).

C Additional Ablation Study

Task key representation and codebook depth for other incremental learning setups. As shown in Tab. 17, we provide the lookup accuracy in other incremental learning setup. Using max-pooling consistently achieves desirable, if not optimal, selection accuracy.

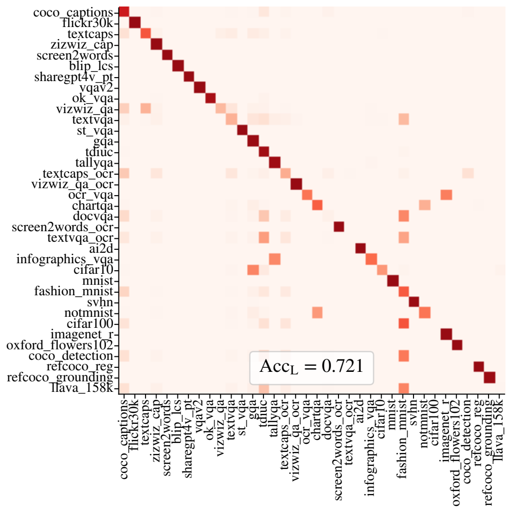

(a) `[CLS]`; l=2

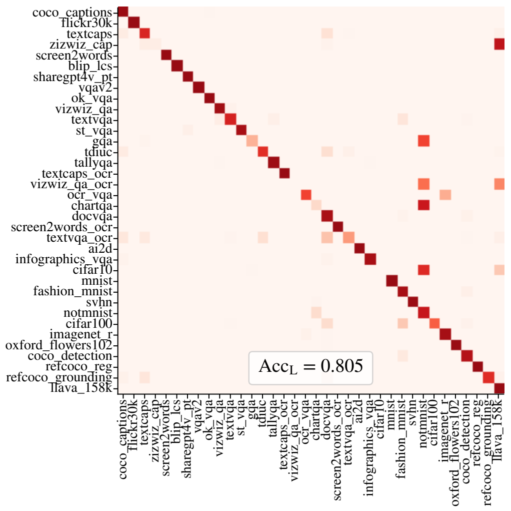

(b) `[[CLS]; [EOS]]`; l=0

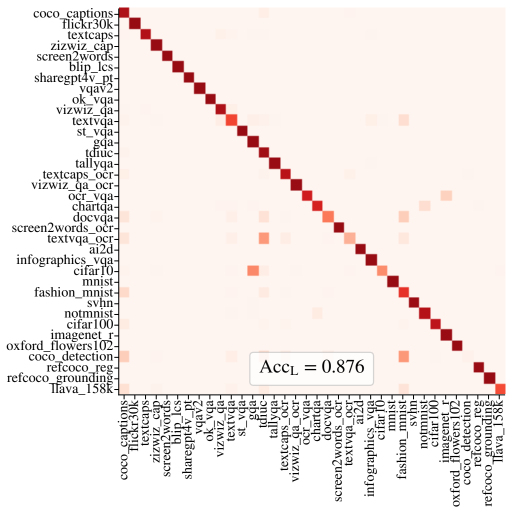

(c) `[[CLS];` max-pooling`]`; l=0

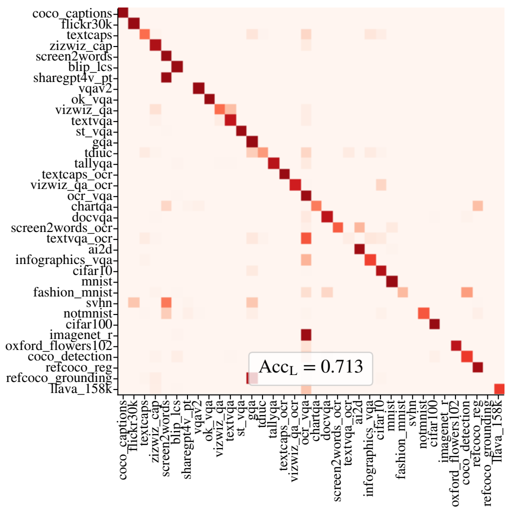

(d) CLIP Radford et al. (2021); l=0

Figure 9: **Confusion matrix** for application-incremental learning across 8 applications (left) and 36 datasets (right).

Confusion matrix. In Fig. 8, we provide the confusion matrix for application-incremental learning experiments on 8 applications. The lookup accuracy is 91.1%, which is -5.8% lower than application-incremental learning on 36 datasets. Specifically, COCO Lin et al. (2014) and Flickr30K Young et al. (2014) datasets in the captioning application are mistakenly recognized as the VQA application, leading to undesirably low performances. This is potentially due to the shared task key representation for the captioning application being dominated by BLIP-LCS Li et al. (2022); Liu et al. (2023) and ShareGPT4V-PT Chen et al. (2023a) given the prevalence in example amount (1.4M *v.s.* 142K).

D Limitations and Potential Negative Impact

D.1 Limitations

Requirement for Task ID at Training Time. One limitation of the proposed method is the requirement of the training task ID for task codebook adaptation. The adaptation process relies on identifying and retrieving the correct set of parameters at training time for a given task. This requirement poses a significant challenge in scenarios where the task ID may not be readily available or easily determined. It leaves for future work to explore training without the need of the task ID.

Memory Overheads. Although we aim to mitigate catastrophic forgetting without significant memory overheads, the scalability of the task codebook and its efficiency in a scenario with an extremely large number of tasks need further exploration. There could be practical limitations related to the memory footprint.

Generalization across Diverse Domains. While we evaluate the method across a broad range of tasks, the real-world applicability of the model's adaptability and efficiency in continuously evolving or extremely diverse domains remains to be examined. There might be domains or specific types of tasks where the proposed method does not perform as effectively.

D.2 Potential Negative Impact

Biases. There is a risk of the model inheriting or amplifying biases present in the training data. The continuous adaptation process might not adequately address these biases, potentially perpetuating them in downstream applications.

Privacy. The adaptation of models to specific tasks could involve processing and storing sensitive or personal information, especially in applications that deal with user-generated content. If not properly handled, this could lead to privacy breaches and violations of data protection regulations.

Environmental Impact. Training and adapting large models require significant computational resources, which can have a considerable environmental footprint. Incremental adaptation could exacerbate this issue by requiring frequent retraining on new tasks.